INVESTIGATION AND OPERATION OF A CARBON DIOXIDE TEA LASER

William Frederick Bassett

NAVAL POSTGRADUATE SCHOOL
Monterey, California

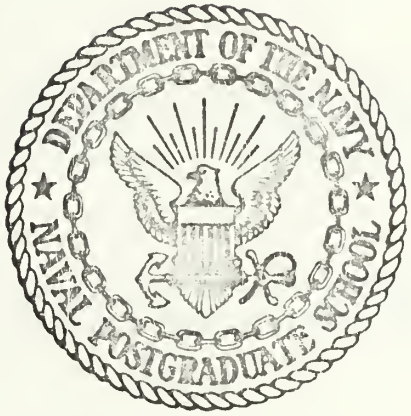

THESIS

INVESTIGATION AND OPERATION
OF A
CARBON DIOXIDE TEA LASER

by

William Frederick Bassett

Thesis Advisor: N. M. Ceglio

June 1973

Investigation and Operation of a Carbon Dioxide TEA Laser

by

William Frederick Bassett
Lieutenant, United States Navy
B.S., Purdue University, 1968

Submitted in partial fulfillment of the
requirements for the degree of

MASTER OF SCIENCE IN PHYSICS

from the

NAVAL POSTGRADUATE SCHOOL
June 1973

ABSTRACT

Lasing has been achieved at 10.6 microns using a double discharge CO_2 TEA configuration. The double discharge configuration utilizes three electrodes. The third, "trigger," electrode in this particular device consists of glass encapsulated nichrome wires. The third electrode is responsible for corona formation--the dominant preionization mechanism. A parametric analysis of the discharge was conducted. The discharge was found to be dependent on the gas mixture, the gas flow rate, the voltage rise time and the voltage pulse shape. It was found that satisfactory discharge operation leading to lasing was limited to a very small region of parameter space having a helium percentage of not less than 90% (with 5% CO_2 and 5% N_2), and a rise time on the order of 3 μsec. Lasing action yielded 5 joules/pulse. The energy was limited by the optical components used, and it is felt that the energy can be increased to approximately 18 joules/pulse using different circuit parameters in conjunction with improved optical components.

TABLE OF CONTENTS

TABLE OF SYMBOLS AND ABBREVIATIONS

(No/Ltr/No)	Indicates shot number and date appropriate data was taken
V_o	Voltage applied across Marx generator
I_{max}	Maximum Discharge Current
V_{max}	Maximum Discharge Voltage
I^*_{max}	Maximum Discharge Current achieved prior to arc formation
V^*_{max}	Maximum Discharge Voltage achieved prior to arc formation
τ_r	Rise time of current pulse
τ_f	Arc formation time

I. INTRODUCTION

Lasing has been achieved at 10.6 microns using a double discharge CO_2 TEA configuration. In addition, a thorough investigation of the discharge has been carried out. This thesis reports the results of that investigation and details the efforts leading to the achievement of the laser output. More specifically, the details of the investigative efforts, the output characteristics of the laser and the limitations to the present configuration are covered.

Chapter two details the changes that were made to the cavity which had been built and used for preliminary investigative work at the Naval Postgraduate School. It also describes a new cathode-trigger design which was built but not experimented with and briefly discusses the parameters of the optical cavity.

Chapter three discusses the preliminary investigations which were carried out and relates previous findings regarding the physics involved in spark formation to the operation of a double discharge electrode configuration. During the preliminary investigation, corona formation near the surface of the sawtooth cathode rather than photoionization was established to be the dominant preionization mechanism at work in this system. Some research was also conducted which established that the operation of the laser was very sensitive to the addition of even small amounts of gas additives to the $He/CO_2/N_2$ gas mixture.

A parametric study was conducted to find the relationships between the seemingly important parameters such as the applied voltage, the maximum discharge voltage, the maximum discharge current, the circuit rise time and the helium percentage of the gas mixture. The study revealed that the maximum attainable discharge current, and subsequently the maximum power, were strongly dependent on the helium percentage of the gas mixture and the rise time of the circuit. This dependence was found to limit satisfactory operation to configurations with rise times on the order of 3 μsec $\pm$ approximately .5 μsec. Perhaps more significantly, it was found that satisfactory operation could not be achieved with gas mixtures comprised of much less than 90% He. This greatly restricts the capability of the system.

Investigation showed that under good discharge conditions the maximum current through the plasma exhibited a strong dependence on the applied voltage. The voltage across the plasma under the same conditions appeared to be independent of the applied voltage. The voltage, on the other hand, showed a strong dependence on the percentage of helium present in the gas mixture. The maximum discharge voltage increased with decreasing helium content.

The value of $(E/p)_{max}$ was looked at for helium percentages ranging from 95% to 85%. This quantity was found to vary strongly with He%. The values found ranged from 8.8 V/cm·torr at 95% He to 12.9 V/cm·torr at 85% He. Using

$(E/p)_{max}$ = 8.8 V/cm·torr, the electron drift velocity was calculated to be on the order of 9×10^6 cm/sec and the electron density on the order of 10^{12} cm^{-3}.

Finally, the discharge resistance was looked at as a function of time. It was found that in general as the helium content of the gas mixture was increased, the minimum value of the discharge resistance decreased. In addition, the discharge resistance tended to remain low for a longer period of time for helium rich mixtures. This is the same "window effect" that has previously been reported in Ref. 2.

The preliminary lasing investigations carried out to date yielded an output of 5 joules/pulse from a discharge condition yielding 175 joules in the discharge. Lasing operation has thus far been limited by the quality of the optics and instability of the optical bench and mirror mounts. Both of these limitations can be easily overcome. Optimizing the optics should readily increase the output energy to about 11 joules/pulse.

The power in the laser pulse was measured as a function of time. It was characterized by a large amplitude peak of approximately .4 μsec duration with a tail lasting approximately 2 μsec.

The discharge condition which has thus far been used for lasing is not the optimum discharge energy condition but was chosen for experimental use because of its reproducability. Utilization of another discharge condition

which has coupled as much as 285 joules/pulse into the discharge along with optimization of the optics should yield output energies as high as 18 joules/pulse.

II. CONSTRUCTION

A. MECHANICAL

1. Changes

Although the general construction of the laser cavity was the same as that described in Ref. 2, several changes were made during the course of experimentation.

During the early stages of experimental work, while exploring the operational parameters associated with a 2 cm gap, it was found that there was a tendency for arcing to occur between the exposed portion of the trigger wires and the cathode. At the same time, it was found that the most likely mode of failure for the glass enclosed trigger wires was through fracture at the end of the glass rods. Fracture at this location was attributed to the cathode-trigger geometry which caused large electric field concentrations at the tips of the nichrome trigger wires. It was found that by encasing both the exposed wires, along with the copper bar and incoming trigger connection, and the ends of the glass rods in an RTV silicone rubber compound both of these problems could be satisfactorily overcome. Of the many RTV silicone rubber materials available, the material chosen for use was a dimethyl RTV compound (G.E. RTV-602). G.E. SRC-05 was used as the catalyst in preparation of the RTV compound. Typical electrical properties of G.E. RTV-602 which made it useful for this insulating application were:

Dielectric Strength (0.075" thick) 500 V/mil

Volume Resistivity 1×10^{14} ohm·cm

Prior to application of the RTV compound, the surface was cleaned using acetone and then primed with G.E. SS-4004 silicone primer. The areas to be covered were encapsulated by pouring the RTV compound into lucite forms.

The incidence of fracture at the ends of the trigger wires, and the resultant arcing at these points, was further reduced by reversing the polarity of the applied voltage and then leaving the trigger wires and anode at ground potential while swinging the cathode to a negative potential. This was done by taking a positive voltage from the power supply. The polarity of the voltage was reversed by the Marx generator and a negative potential applied as desired. This configuration reduced the electric field intensity at the ends of the trigger wires.

In an effort to isolate the cathode assembly, the physical arrangement of the anode and cathode-trigger assembly was inverted from that shown in Ref. 2. The cathode-trigger assembly was suspended from the top of the cavity and the anode fixed at the bottom of the cavity.

Experimental work showed that the two outlet ports for the gas mixture, described in Ref. 2, were unnecessary to vent the gas to the atmosphere. It was found that by changing the outlet ports to inlet ports satisfactory gas flow could be achieved while operating with a slight

overpressure in the cavity and venting through the cracks inherent in the cavity corners, etc.

2. New Design

A second cathode, similar to that described by Pan in Ref. 3, was built but has not been tested. This cathode-trigger assembly is shown in Figures 1 and 2.

The dimensions of the lucite base plate are 40" x 12" x 1". This base plate was designed to interface with the anode and cavity which are currently in use. The cathode assembly consists of 131 aluminum cathode blades constructed of 1/64" thick aluminum. The blades are 4" long and 1" high and have been constructed without sharp corners, as shown in Figure 2, in order to reduce the electric field intensity in these regions. The blades are separated by 1/4" lucite spacers and are electrically connected by two threaded brass rods.

As in the sawtooth design, the trigger assembly consists of glass encased nichrome wires. The glass rods are 7/32" in diameter and are approximately 7 5/16" in length. This design uses 130 trigger wires positioned between the cathode blades with the trigger wire at the same height as the edge of the cathode blade and parallel to the edge of the cathode blade. The height of the cathode blades and the positioning of the trigger wires is critical.

With this cathode-trigger assembly a greater corona is expected. This expectation is based on geometric improvements over the original design. The geometry of this

design allows the trigger wires to be placed in the closest proximity to the sharp edges of the cathode blades, the orientation which allows the greatest electric field and maximum corona formation.

B. OPTICAL

An analysis of the resonant cavity for the CO_2 TEA laser was included in Ref. 2. The back mirror may be either a flat polished copper mirror or the same 4" diameter, three meter radius of curvature polished copper mirror used previously. Copper is, of course, a good choice for this mirror because of its nearly perfect,98.8%, reflectance of radiation above .9 micron wavelength [3].

As cited in both Ref. 1 and Ref. 2, either of two methods may be used to satisfactorily achieve output coupling of the laser energy. First, and most simply, a mirror constructed of material such as polished copper which has a high reflectance may be used if a hole is drilled in the center of the mirror. When used in a high gain system with a hole size small compared to the mode spot size, this method is as effective as the use of a partially reflecting mirror; the method to be discussed later in this section. In addition to the flat circular polished copper mirror with a .79mm output hole cited in Ref. 2, mirrors of the same size and surface finish were machined with output holes graduated in size from 1/8" to 1".

The second method of output coupling is through use of a solid back mirror fabricated from a material which is only partially reflecting to radiation of the wavelength of interest--10.6 microns in this case. The transmission coefficient of the mirror must be sufficient to achieve optimum output without unduly damping laser oscillation in the cavity. A 4-1/2" diameter germanium mirror 15/32" thick was selected for use as the front mirror. In general, germanium is a good material for use in transmitting components for several reasons. (1) It has a high thermal conductivity which allows efficient cooling and reduces the chance of damage at high power operation. (2) It has relatively low absorption. The absorption of germanium at 10.6 microns is dependent on both purity and temperature. Typically, the germanium used for optic applications will absorb between .7% and 1% per mm. (3) Germanium can be polished to a high quality optical finish.

Typical material properties of germanium are shown below in Table I.

TABLE I
Material Properties of Germanium

Refractive Index at 10.6 microns	4.0
Thermal Conductivity (cal/cm sec ^{o}C)	0.14
Thermal Diffusivity (cm^2/sec)	0.35
Specific Heat (cal/g ^{o}C)	0.074
Density (g/cc)	5.33
Thermal Expansion Coeff. ($10^{-6}/^{o}C$)	6.1

Typical spectral data for germanium is shown in Figure 3. It can be seen from this figure that the transmission at 10.6 microns is approximately 45% [5].

When the germanium mirror was used, an arsenic trisulfide lens was used to focus the output beam. The spectral data for arsenic trisulfide is shown in Figure 4 [6].

III. EXPERIMENTAL RESULTS

A. PRELIMINARY INVESTIGATIONS

1. Discharge Geometry

As mentioned previously in the section dealing with construction, the early experimental work with a 2 cm gap showed a tendency for arcing to occur, particularly between the cathode and the ends of the trigger wires. This tendency, as might be expected, was greatest in the regions of high field concentrations - the ends of the trigger wires being the highest such region. It was found that arcing, causing damage to the glass rods, occurred at some voltage below 50 kV. The application of G.E. RTV-602 compound, with its insulating properties, was a first step in eliminating the problem. In addition, it was felt that this tendency toward arcing could be further reduced by letting the anode and trigger wires remain at ground potential while swinging the cathode to a high negative potential. This had the effect of reducing the field concentrations at the ends of the trigger wires, and, at the same time, it was expected that the change would have no effect on the electric fields within the anode-cathode gap. This was found to be true in further experimental work with the 2 cm gap. The operation was found to be very similar to operation before the change with the exception that, as desired, the tendency to arc at the ends of the trigger wires was eliminated.

Fracture of the glass tubing surrounding the trigger wires had not been completely eliminated at this point. Several fractures occurred after the indicated changes were made; however, they occurred in regions close to the sharp cathode edges and occurred as a result of higher voltages i.e. voltages of approximately 50 kV. It is not surprising that this was the region of greatest fracture incidence since following the indicated changes these were the regions of highest field concentrations.

2. High Voltage Search

a. Motivation

Following this work with the discharge geometry, a good deal of effort was expended in searching for a high voltage regime that would result in a uniform, reproducible discharge condition. Several published works including Ref. 7 by Laurie and Hale, Ref. 8 by Rampton and Gandhi and Ref. 9 by Pearson and Lamberton indicated that the desirable operating regime was bounded not only on the high end by some arcing potential but also on the low end. This is surprising and is very different from operation of a two electrode gap which, for a given set of conditions, exhibits one arcing threshold. It must be pointed out that these three papers dealt with laser electrode configurations unlike the one of interest here. Figure 5 is a reproduction of Figure 6 taken from the paper by Pearson and Lamberton. As can easily be seen, their results show that there is an operating regime that has both well defined upper and lower

limits beyond which their experimentation showed that arcing inhibited laser action. They found that the lower limit was defined by a single bright arc which they claimed was probably related to the dc breakdown potential while it appeared that at the higher voltage limit a glow-to-arc transition occurred since a bright arc superimposed upon a uniform discharge was observed. Laurie and Hale, in their paper dealing with the operating characteristics of a pin-electrode CO_2 TEA laser, found that with regard to the laser output the energy increased and the frequency of bright arcs decreased with increasing voltage, again, indicating some lower boundary condition. Similar findings were presented by Rampton and Gandhi in Figure 7 of their paper. They found that the effect of localized arcing increased with decreasing voltage, all other parameters being held constant.

As previously stated, the electrode configurations used in the experimentation cited in these references were quite different from the double discharge configuration considered here. Nevertheless, it was felt that it would be useful to conduct an investigation to determine whether or not an operating region with both a well defined upper and lower boundary could be found for the double discharge laser. In an unsuccessful effort to find such a high voltage regime, voltages ranging from 15 kV to 45 kV, corresponding to electric fields in the 2 cm gap of 7.5 kV/cm to

22.5 kV/cm, were applied. Pearson and Lamberton had found that the upper glow regime onset occurred at values of electric field ranging from 7.7 kV/cm to 20.8 kV/cm depending on the helium percentage of their gas mixture while Laurie and Hale found onset values ranging from 9.4 kV/cm to 21.8 kV/cm and Rampton and Gandhi found values of 8 kV/cm to 14 kV/cm. It was concluded that arcing with the present double discharge configuration serves only to delineate an upper boundary for the operating regime. The lower boundary is not as pronounced and is marked only by a degradation and then cessation of operation.

b. The Three-Point Effect and Photoionization

In 1926 C. E. Wynn-Williams published an article entitled "An Investigation into the Theory of the Three-Point Gap," [10] in which he presented the results of his experimentation into the phenomenon known as the three-point effect. The phenomenon of the three-point effect is as follows. Consider two electrodes of a spark gap connected to an impulsive high potential apparatus, for any given set of conditions there will be a definite maximum width of the gap, depending on the peak voltage, the dimensions of the electrodes, etc., for which a spark can pass regularly. If the gap width is increased, the other conditions remaining the same, the spark will not pass. If a third pointed electrode is brought near one of the other two electrodes the spark might again pass across the main gap. It was found that the third electrode could be either

isolated or at the same potential as one of the other electrodes. It could not, however, be at ground potential. Wynn-Williams found that it did not seem to make any difference which of the main electrodes the third approached unless one was grounded in which case the other must be approached for the phenomenon to be observed. The main gap spark was accompanied by a corona discharge between the third electrode and its neighboring main electrode. It was found that the corona discharge might be either a visible (pilot) discharge or a silent discharge. Even in a dark room, the silent discharge could not be observed. Wynn-Williams concluded that the three-point effect was caused by the ionization of the gas in the main gap by radiation emitted by the pilot or silent discharge. The radiation responsible for the effect was thought to be Entladungstrahlen which lies in the region of wavelength less than ultra-violet and greater than soft x-rays. He also concluded that disturbances in the field, passage of ions into the gap, or photo-electric effects produced by the radiation or by ultra-violet light, while possibly assisting in, are not essential for, the three-point effect.

It can then be seen that the presence of the third electrode has a very real effect on the behavior of the discharge. While the phenomenon described by Wynn-Williams is very different from that described in Refs. 7, 8, and 9, it should be pointed out that the electrode configurations described in those three references are all

multi-electrode configurations satisfying the criterion established by Wynn-Williams that the third electrode must be able to "see" the gap either directly or by reflection. In the configuration used by Pearson and Lamberton, the third electrode is a fine tungsten wire. In the configurations used by Laurie and Hale and by Rampton and Gandhi the third electrode may be any of the pins satisfying the above criterion.

Streak photograph analysis showed photoemission from the discharge between the tungsten wire and the anode to be the mechanism responsible for discharge initiation in the solid cathode laser design used by Pearson and Lamberton. The photons then cause ionization at the cathode surface and the discharge begins from the cathode.

The preionization mechanism responsible for the discharge in the pin type lasers is not as clear. However, due to the small surface area involved in such a system, the mechanism is more than likely a volume photoionization attributed to the radiation from the "third electrode" discussed by Wynn-Williams.

It is speculated here that strong photoionization processes, which onset at high voltage, may alter arc formation times in the laser discharges of Pearson and Lamberton, Laurie and Hale and Rampton and Gandhi. The alteration of the arc formation time at high voltage may then lead to the two arcing thresholds that they observed. This mechanism will be discussed in greater detail in the following sections.

c. Theory of the Electric Spark

A brief discussion of spark formation is in order at this point. In their book, The Mechanism of the Electric Spark, [11] published in 1940, Meek and Loeb described the growth and propagation of an electric spark. The application of sufficient voltage to a two electrode gap will cause an electron avalanche from the cathode to the anode with the resultant growth of a streamer from the anode leading to a spark channel. The time that it takes a spark to develop once the avalanche has begun at the cathode is the formative time lag (τ_f). The formative time lag is inversely proportional to the over voltage applied to the gap and thereby to the applied fields. The streamer is a conducting plasma with an ion space charge localized at its tip. The streamer advances toward the cathode as a sharply pointed "finger". The geometry of the leading point of the streamer, the localized space charge, plus the effectively decreasing anode-cathode distance at this point leads to a large space charge electric field in the region of the point. This space charge field exceeds the applied field to the gap.

The three configurations that have been discussed are fast systems characterized by rise times on the order of 100 nsec and peak widths of 100-300 nsec. In the absence of any preionization or in the event of insufficient preionization, the very large space charge fields associated with streamer growth make it highly possible that the

formative time lag will be less than the rise time of the voltage i.e., a spark will form in a time that is short compared to the time that the voltage can reach its maximum value and then get back down to a value too small to support breakdown. As the preionization is increased, many avalanches will begin from the cathode leading to the growth of many streamers from the anode and an attendant decrease in the space charge electric field concentration at the streamer tips. The decrease in space charge field concentrations is explained as follows. The many streamers will have a homogenizing effect on the space charge distribution and the associated field will approach a flat plate configuration. With the space charge field reduced due to strong photoionization, it would be possible for τ_f to increase to a value greater than the discharge pulse width (τ_d) so that the gap would no longer break down in a localized arc. As the voltage across the gap is increased, a point will eventually be reached at which although sufficient preionization is provided to create the homogenizing effect just described, the overvoltage will be sufficient to again reduce τ to a value equal to or less than τ_d returning the configuration to an arcing regime.

So, we may explain the double arcing boundary in the following way. The arcing regime at low voltage is associated with the usual breakdown experienced in two-electrode experiments. Photopreionization from adjacent electrodes is not important here because the applied

voltages are too low. The arc formation time is shorter than the discharge time. As the voltage is increased, photopreionization of the gap from adjacent electrodes increases thereby increasing the arc formation time. When the voltage is increased to a level at which $\tau_f > \tau_d$, arcing no longer occurs during the discharge. This is the lower threshold of the glow regime. Now, as the voltage is further increased, the space charge homogenization effects of the photopreionization will eventually be offset by the growing applied field. That is, once the ideal "parallel plate" configuration for the space charge field is established by photoionization, further increases in the externally applied field will cause a linear increase in the space charge field in the gap. Thus, with further voltage increase, the arc formation time again begins to decrease. The applied voltage at which $\tau_f < \tau_d$ defines the beginning of the upper voltage arcing regime.

B. PREIONIZATION IN THE DOUBLE DISCHARGE LASER

In considering the double discharge laser configuration of interest here, it is important to note that the characteristic rise time for the current ranged from 1 μsec to 3.6 μsec rather than being on the order of 100 nsec. It might then be speculated that a different mechanism is responsible for a good glow condition in this system. It is then desirable to determine what mechanisms contribute to the achievement of a good glow condition in this system.

There are three possible preionizing mechanisms to be considered: (1) corona formation near the surface of the sawtooth, (2) photoionization of the surface of the flat electrode, and (3) volume photoionization of the gap. Since the photon range is on the order of 5 cm to 6 cm [10], none of these mechanisms can be ruled out solely on the basis of geometric considerations.

In an effort to experimentally isolate the responsible mechanism, both positive and negative potentials were applied to the sawtooth. Application of 22.5 kV across the 2 cm gap containing gas mixtures of 95% and 80% He gave different results for the different polarities. When the sawtooth electrode was given a positive potential with respect to the flat electrode, consistent arcing occurred; however, when the polarity was reversed a uniform glow discharge was consistently observed.

In concluding which preionization mechanism contributed to the achievement of a uniform glow condition in the double discharge laser, several points must be made. It would have been expected that if volume photoionization were the dominant preionizing mechanism, operation would have been independent of electrode polarity. Similarly, photoionization of the flat surface would favor the positive sawtooth configuration and corona formation near the sawtooth would favor a negative sawtooth. Since it was found that glow operation was attainable only with the latter arrangement, it was

concluded that corona formation near the sawtooth was the preionizing mechanism contributing to the achievement of a uniform glow discharge.

C. CIRCUIT INVESTIGATIONS

1. Variation of the Voltage Slope (dV/dt)

The research done by both Pan [3] and Dumanchin [12] has indicated that dV/dt, the time rate of change of the voltage applied to the gap, is a relevant parameter to be considered with regard to the operation of double discharge CO_2 TEA lasers. In an effort to look at the results of varying this parameter, the operation of the two circuits shown in Figure 6 was observed. The other relevant parameters such as voltage rise time (τ_r), the maximum voltage across the gap and the gas mixture in the cavity were held constant to isolate the effect of dV/dt.

Figure 7 shows the shape of the voltage pulse appearing across the gap for both circuits prior to breakdown as well as dV/dt for both cases. The figures are not meant to indicate the shape of the voltage or of dV/dt after breakdown of the gap. The pulse shapes, as presented, are idealized shapes. As such, they are accurate only until such time as the impedance of the gap is reduced to a value comparable to that of R or C_2 at which time the simplification of the gap as an open circuit is no longer valid.

The distinguishing characteristic of the two circuit configurations is the manner in which the voltage across the

gap varies with time. For the fast circuit, the voltage varies as $V_f \alpha V_o \sin \omega t$. Initially, this voltage increases rapidly. The rate of increase then decreases with time. Conversely, in the circuit used by Pan, a slowly increasing voltage which varies as $V_p \alpha V_o(1-\cos 2\omega t)$is initially applied across the gap. The maximum rate of increase occurs at T/4 ($T = 2\pi/\omega$) a time corresponding to one-half the rise time of the circuit. At this time, the rate of increase of the voltage across the gap is equivalent to twice the maximum rate of increase for the fast circuit.

It should be noted that the above comments regarding the shape of the voltage pulse and the time rate of change of the voltage for the fast circuit are based on the use of an underdamped configuration. In the case of an overdamped circuit, the voltage pulse initially rises as sinh ωt and the derivative shape varies initially as cosh ωt. Since sinh ωt and cosh ωt initially rise more rapidly than sin ωt and cos ωt respectively, the conclusions reached later in this section are valid in either the overdamped or the underdamped case.

It was found that it was possible to achieve a weak glow discharge with the fast circuit. The glow was achieved in an 80% helium gas mixture using a rise time of 1 μsec. The discharge voltage was only 10 kV and the current only a few hundred amperes (11/MR/22). An effort to increase the discharge voltage and current by increasing the applied voltage caused arcing. Using Pan's circuit with the same

gas mixture and the same rise time, a discharge voltage of 20 kV and a discharge current of 700 amperes was achieved (6/N/3). Again, efforts to increase these values by increasing the applied voltage caused arcing to occur.

A more direct comparison of the two circuits was found when operating with a 95% He mixture and a rise time on the order of 1.2 μsec. Pan's circuit produced a glow with an associated current of 1100 amperes for a voltage across the gap of 13 kV (19/N/3). At this condition, a slight increase in voltage caused arcing. Operation of the fast circuit at these conditions was impossible since arcing occurred for discharge voltages on the order of 10 kV (1a/MR/22).

In general it can be stated that the use of Pan's circuit yielded both high currents and uniform discharges. This was not true of the fast circuit. It therefore does not appear that a powerful, uniform discharge sufficient to produce lasing action in the double discharge device is possible with the fast circuit in the rise time regime of .7 μsec to 3.6 μsec which was investigated.

Both Pan [3] and Dumanchin [12] were unsuccessful in their attempts to use the fast circuit to achieve spatially uniform breakdown of the gap in preparation for lasing. Pan stated that, "It is important to note that although the rise and fall time criteria were followed, some circuits did not give expected performance. The parameter that was varied with these circuits was the slope of the high voltage

pulse near the beginning. When the voltage pulse rose rapidly, we observed a sharp current pulse, with a full width at the base, of less than 0.5 μsec in the trigger discharge and no main discharge current until arcing occurred. Even when the arcing in the main gap occurred, several micro-seconds after the start of the voltage pulse, no corona current was observed in the trigger gap after the initial spike. The performance of the D^3 (double discharge device) improved when the initial voltage pulse slope was decreased. In that case we observed a slow-rising trigger discharge current, which continued for about 2 μsec without the initial spike, and a large main discharge current. Thus, in addition to the rise and fall time requirements, the initial slope of the high voltage pulse must be kept small."

There seem then to be two possible explanations why satisfactory operation can be achieved with Pan's circuit but not the fast circuit. First, as Pan stated, perhaps no corona is formed with the fast circuit. Secondly, perhaps the shape of the voltage pulse is important in determining the rate and degree of space charge build up in the gap. Our results appear to support the latter explanation rather than the former.

The experimental data previously presented are in opposition to Pan's statement that no corona is formed when the fast circuit is used. With the trigger inactive, it has not been possible to achieve a uniform glow discharge

with either the fast circuit or Pan's circuit. Operation of the circuits with no trigger has produced either no discharge or arc formation regardless of the other circuit parameters. The presence of a uniform glow region, however small, with the fast circuit when the trigger is activated points to the formation, to some extent, of corona.

It appears reasonable that space charge build up is the differentiating factor in the operation of the two circuits. The Townsend criterion for formation of a self-sustaining avalanche in a gap is that $\gamma e^{\alpha\delta} \geq 1$ where γ is the probability that a positive ion will liberate a new electron from the cathode and $e^{\alpha\delta}$ is the number of positive ions produced by an initial electron in going distance δ [11].

Experiment has shown that both γ and α are related to the voltage applied to the gap through a functional dependence on E/p where E is the electric field strength and p the pressure in the gap. There is then some critical voltage (V_c) which corresponds to the equilibrium condition $\gamma e^{\alpha\delta} = 1$. For a voltage greater than this critical voltage space charge build up is experienced in the gap. Figure 7 shows that any time $t < T$ the fast circuit gives a greater voltage across the gap than does Pan's circuit. Therefore, for any value of $V_{max} > V_c$ the fast circuit operates in the region of space charge build up for a longer period of time than does Pan's circuit. This situation leads to a higher probability of arcing for the fast circuit.

The requirement for a glow discharge without arc formation is that the gap voltage (V) must be greater than V_c for a time less than the arc formation time. Pan's circuit is more appropriate for glow discharge operation because for a given V_{max} and a given τ_r its voltage spends less time above V_c than the voltage of the associated fast circuit. Nevertheless, there can obviously exist appropriate V_{max} and τ_r for the fast circuit such that $V > V_c$ for a time less than τ_f. Under such conditions, the fast circuit will lead to a glow discharge in the gap. We have indeed demonstrated that such a glow condition does exist using the fast circuit.

2. Effect of L^*

Early in the course of the experimental work, when operating with a 2 cm gap, great difficulty was experienced in getting currents greater than 1200 amperes under any discharge conditions using Pan's circuit (Figure 6). It was thought that by changing Pan's circuit to that shown in Figure 8 through the addition of L^* this problem could be overcome. The purpose of L^* was to initially reduce the current, and therefore the energy, lost through R, the drainage resistor. When L^* is not in the circuit, the current I_R through the resistor is similar to that shown in Figure 9a. For this configuration $V_x = I_R \cdot R$. As V_x increases, I_R increases linearly.

The addition of L^* changes the relationship between the voltage V_x and the current through the resistor I_R.

Now, $V_x = I_R R + L^* dI_R/dt$. It can easily be seen that, for a given V_x, I_R is less when L^* is added to the circuit than when Pan's circuit is used. This is particularly true during the initial stages of the pulse when dI_R/dt is large. The resulting pulse shape of I_R is shown in Figure 9b.

The expected results were found experimentally. A reference shot was fired with $L^* = 0$ using the following parameters:

V_o = 22.5 kV Energy in = $\frac{1}{2} C_m V_o^2$ = 42.27 joules

C_m = .167 μf $He\%/CO_2\%/N_2\%$ = 91.75%/4.927%/3.33%

C_2 = .016 μf

L = 7.9 μh

C_t = 0

A good glow with some fingers was observed yielding:

I_{max} = 1200 amperes (2/MR/27)

$I_{R\ max}$ = 4400 amperes

V_{max} = 20 kV

Total Energy in discharge = 9.14 joules

Efficiency = .2162

Addition of L^* 11.5 μh yielded the following:

I_{max} = 1600 amperes (5/MR/27)

$I_{R\ max}$ = 4200 amperes

V_{max} = 21 kV

Total Energy in discharge = 20.85 joules

Efficiency = .4932

As can be seen I_{max} was increased, I_{Rmax} decreased and the total energy into the discharge, and therefore the efficiency was increased.

At this time and throughout the course of the experimental work other minor circuit changes were experimented with. These consisted mainly of adding tuned L-C configurations to the circuit in series with the drainage resistor. None of these investigations were extensive and none of them appeared to be too promising.

The L^* circuit was used repeatedly but never extensively investigated until late in the work with the 6 cm gap. At that time an extensive effort was again made to optimize the L^* circuit. Again, a reference shot was fired using Pan's circuit with the following parameters:

V_o = 60 kV Energy in = 660.6 joules

C_m = .367 μf

C_2 = .05 μf

L = 30.5 μh

R = 10.7 ohms

$He/CO_2/N_2$ = 90%/5%/5%

A powerful uniform discharge was obtained yielding the following:

I_{max} = 3550 amperes (46/MA/12)

V_{max} = 63 kV

P_{max} = 21.1 x 10^7 watts

Total Energy in Discharge = 285.34 joules

Efficiency = .432

The addition of L^* yielded the following:

I_{max} = 3800 amperes (22a/MA/13)

V_{max} = 53 kV

$P_{max} = 19.5 \times 10^7$ watts

Total Energy in Discharge = 265 joules

Efficiency = .401

So, the improvement seen at the 2 cm gap while operating with lower voltages and currents was not universal. The total energy delivered to the discharge for the conditions with and without L^* at 6 cm gap is the same to within experimental uncertainty.

D. INVESTIGATION OF THE EFFECTS OF THE TRIGGER

The circuit shown in Figure 10 was used to carry out an experimental procedure aimed at quantifying the effects of the trigger. The trigger was made inactive by connecting the high end of the trigger capacitor (C_t) to the cathode. The active trigger circuit was the same circuit as that previously referred to as Pan's circuit, Figure 6.

The following investigative procedure was used. The values of C_m, τ_r , R and the He% were established and held constant throughout the entire investigation. With the trigger active, V_o, the potential across the Marx generator at the time of firing, was slowly increased until arcing occurred. The trigger was then made inactive and the procedure repeated.

In general, the following behavior was observed. When the trigger was active, a uniform glow discharge was obtained and I_{max}, the maximum value of current achieved during the discharge, increased with V_o until arcing occurred.

Values of I_{max} ranging from 1000 amperes to 3000 amperes were not unusual. Arcing occurred at a Marx generator voltage $V_o = V_o^*$. It was found that V_{max}, the maximum voltage across the gap during the discharge, was generally less than V_o and appeared to be independent of V_o. This will be discussed in greater detail in a later section of this paper.

With the trigger inactive, at sufficiently low voltages, no visible discharge was observed. As the voltage (V_o) was increased, minute streamers began to appear. They appeared at the anode edges and grew toward the cathode as shown in Figure 11. The streamers were confined to the edges of the electrodes. The streamers were pink in color and grew from white "spots" on the anode. The pink color of the streamers was associated with the nitrogen in the gas mixture. The length of the streamers increased with increasing V_o until they completely bridged the anode-cathode gap. The number of streamers growing from the anode appeared to correspond to the number of ridges on the cathode. The shape of the streamers closely matched the expected "bowed out" shape of the field lines associated with the edges of a parallel plate capacitor. Increasing V_o led to increasing brightness of the streamers, then to the appearance of white spots where the streamers contacted the cathode and finally to the development of one single powerful arc.

It was found that under inactive trigger conditions V_{max} varied linearly with V_o. This was not unexpected since

the observed discharge was extremely weak except when arcing occurred. The precise value of V_{max} for any given V_o' was, of course, determined by the value of R used in the circuit. It was not unusual to find values of $V_{max} > V_o$ for sufficiently large values of R. The values of I_{max} observed for the inactive trigger condition were extremely small, less than 100 amperes, except when arcing occurred.

In an effort to attach some numbers to the above qualitative discussion, the following results of a typical inactive-active trigger investigation are presented. The parameters common to both circuits were:

Gap Width = 6 cm

C_m = .167 μf

C_2 = .025 μf

L = 18.1 μh

C_t = .004 μf

R = 10.2 ohms

The following gas mixtures were used:

$He/CO_2/N_2$ = 87.5%/6.25%/6.25%

$He/CO_2/N_2$ = 95%/2.5%/2.5%

When V_o was varied, holding all other parameters constant, the following results were obtained:

1. Under inactive trigger conditions, the value of V_o^* (V_o at arcing) was greater when the 87.5% helium mixture was used than when the 95% helium mixture was used. Specifically, for the 87.5% He mixture V_o^*=48 kV while for the 95% He mixture V_o^* =39 kV.

2. The value of V_o^* for the active trigger configuration was found to be well above that observed for the inactive configuration when either gas mixture was used. More precisely, at 95% He with an active trigger V_o^*= 60 kV while with an inactive trigger V_o^*= 39 kV. It is important to note that this data is not meant to imply that the maximum voltage across the discharge gap in an arcing condition, V_{max}^*, is greater with the active trigger configuration than with the inactive trigger configuration. When a powerful discharge occurs in a relatively high helium percentage gas mixture $V_{max} < V_o$. This is caused by the low plasma resistivity across the gap. This is discussed in greater detail in a later section of this paper. Conversely, for the inactive trigger with R=10.2 ohms V_{max} was found to be greater than V_o.

E. INVESTIGATION OF THE EFFECTS OF GAS ADDITIVES

During the course of experimentation, it was often found that when arcing would occur at a given V_o, satisfactory operation could be achieved for that same voltage by increasing the flow rate of the gas mixture into the cavity, i.e., the arcing probability for a given set of discharge conditions seemed to depend on the gas flow rate.

For example, operating with Pan's circuit configuration, Figure 6, with the following parameters:

$$C_m = .367\ \mu f$$

$R = 17.1$ ohms

$L = 18.1$ μh

$C_2 = .075$ μf

$C_t = .004$ μf

He% = 92.5%

it was found that for a gas flow rate of 36,694 cm^3/min a uniform glow discharge was achieved for $V_o = 48$ kV. When the voltage was increased to $V_o = 51$ kV at this same flow rate, arcing occurred. However, by increasing the flow rate to 47,130 cm^3/min, uniform glow discharge operation was achieved at $V_o = 51$ kV (47,48/MA/2).

Results such as these led to a short statistical study to isolate the effect of flow rate on circuit operation. For this study, Pan's circuit was used with the following parameters:

$V_o = 57$ kV (A,B,C/MA/7)

$C_m = .367$ μf

$R = 8.69$ ohms

$L = 30.5$ μh

$C_2 = .075$ μf

$C_t = .004$ μf

He%= 92.5%

It was found that operating with a flow rate of 58,000 cm^3/min gave reproducible glow operation. No arcs were observed with this flow rate. Decreasing the flow rate to 27,614 cm^3/min produced a situation in which 100% of the shots arced.

For an intermediate flow rate (35,700 cm^3/min) 40% of the shots arced while the remaining 60% produced a uniform glow discharge. In all cases three minutes elapsed between shots. During this time, the gas continued to flow.

There appear to be three possible explanations for these results.

1. Increased cooling of the gas mixture due to the increased flow rates.
2. Dynamic effects in the cavity due to the increased flow rate.
3. Increased overpressure in the cavity resulting in fewer impurities in the gas mixture.

Simple calculations will suffice to show that neither number 1 nor number 2 above could be the mechanism leading to improved operation at higher flow rates.

The total volume of the lucite cavity, including the volume occupied by the electrodes is 4826 cm^3. Thus, even the lowest flow rate used in the statistical study replaces all of the gas in the cavity nearly six times during the three-minute waiting time between shots. This is entirely sufficient to insure that each shot, whether with the highest or lowest flow rate, was fired with the same gas temperature.

The highest flow rate used was 58,000 cm^3/min. As previously stated, the gas mixture entered the cavity through five 1/4 inch inlet ports. This produced a flow velocity

into the cavity of 576 cm/sec. For a pulse width of 3μsec then, the distance that a particle would travel due to this streaming velocity would only be on the order of .018 mm. Thus, even for the highest flow rate the dynamic effects produced by the flow rate would be insignificant.

It seems then that the improved operation at higher flow rates can be attributed to the increased overpressure and corresponding decrease in impurities in the cavity at the higher flow rates.

In order to isolate the effect of impurities on the discharge, the following procedure was used. A condition was established which was close to an arcing condition, but which would yield a glow discharge on a reproducible basis. Using Pan's circuit with the following parameters:

C_m = .167 μf

R = 5.8 ohm

L = 7.9 μh

C_2 = .016 μf

He%= 95%

V_o = 22.5 kV

glow discharge resulted in:

V_{max} = 18 kV (10h/MR/28)

$I_{A\ max}$= 1000 amperes

$I_{R\ max}$= 4000 amperes

Approximately .6% impurities were introduced into the cavity in the form of oxygen (O_2) and freon (CCl_2F_2). Introduction

of either gas led to arcing. In the absence of either gas a return to the reference condition above again produced a uniform glow discharge.

Thus, the presence of even small amounts of at least some impurities can have very undesirable effects on the operation of double discharge CO_2 TEA lasers.

Experimental results presented by Deutsch [13], and by Grigoriu and Brinkschulte [14] show that not all additives produce detrimental effects on the discharge or lasing operation. Deutsch investigated the addition of hydrogen to the gas mixture. He found that addition of 3% - 10% hydrogen lead to a more uniform discharge and suppressed the formation of arcs, making possible an increase in the output and the gain by a factor as high as 2. Deutsch felt that two possible explanations for the increased gain were:

1. The promotion by the hydrogen of rapid relaxation of the CO_2 molecules excited to the lower laser level.
2. More efficient utilization of the discharge volume as a result of a more uniform discharge.

He presented the following as possible mechanisms contributing to arc suppression:

1. Cooling of incipient streamers due to the enhanced vibrational energy transfer produced by the hydrogen.
2. An alteration, by the hydrogen, of the chemistry of the discharge by reducing the net dissociation of CO_2 into CO and O_2 and by altering the concentrations of ions in the discharge.

Grigoriu and Brinkschulte similarly found that they could achieve a more uniform glow discharge through the addition of small amounts of xylene to the laser gas mixture. They attributed the improved operation to the low ionization potential of xylene.

Care must be taken not to generalize the results of these experiments. Both experiments were performed using electrode configurations similar to that presented by Pearson and Lamberton [9]. As discussed in an earlier section photoionization is the dominant preionization mechanism in such a configuration. Our laser, on the other hand, is dependent on corona formation near the cathode surface. In addition both lasers were operated with fast rise times (~300 nsec for Deutsch's configuration) and short pulse width (400-600 nsec). Grigoriu and Brinkschulte in fact emphasize that the only critical parameter for improved operation of their system with the addition of xylene was that the current pulse not exceed 400 nsec in width.

Thus while it is interesting to note that some additives produce improved operation of some laser configurations, it can be seen that the systems must be considered individually. Because of the different dominant preionization mechanisms and radically different pulse widths, it is not clear that any benefit would be derived through the addition of either hydrogen or xylene to this system.

IV. DISCHARGE INVESTIGATIONS

A. DEPENDENCE OF I_{max} AND P_{max} ON τ_r AND He%

Figure 12 shows the anode current as a function of both the rise time (τ_r) and the helium percentage of the gas mixture used. In all cases the remainder of the gas mixture was composed of equal parts carbon dioxide and nitrogen. The parameters common to all of the "shots" used to collect the data given in Table II and depicted in Figures 12 through 14 were:

$$C_m = .167\ \mu f$$
$$C_t = .004\ \mu f$$
$$L^* = 0$$

The circuit used was that shown in Figure 6. The values of R and V_o were varied to yield the maximum possible value of I_{max}. The value of I_{max} plotted, then, is the maximum value of current that could be obtained for the given values of He%, τ_r, C_m, C_t and L^*.

It should be noted that the region of variation of both the helium percentage and rise time is quite narrow. The minimum rise time was limited to ~.7 μsec by the operation of the Marx generator. A search of rise times above 3.6μsec was not conducted because the trend of the performance indicated that such a search would be uninteresting at this point, i.e., performance was degrading. Limits on He% were imposed in a similar manner. The operation of this system

TABLE II
Data for Figures 12 through 14

τ_r (μsec)	L (μh)	C_2 (μf)	I_{max} (amp)	V_{max} (kV)	V^* (kV)	P^* (10^7 watt)	He%	Code
1.1	5.7	.008	1200	36	36	4.32	87.5	34/A/11
1.1	5.7	.008	900	44	44	3.06	95	25/A/11
1.6	11.5	.018	500	52	52	2.60	85	10/A/5
1.6	11.5	.018	700	48	40	2.80	87.5	10/A/6
1.6	11.5	.018	1100	40	36	3.96	90	5/A/6
1.6	11.5	.018	1800	44	40	7.20	92.5	37/A/5
1.6	11.5	.018	2400	28	24	5.76	95	53b/A/5
2.1	18.1	.025	1200	45	40	4.80	87.5	15/A/10
2.1	18.1	.025	1900	30	20	3.80	92.5	3/A/10E
2.1	18.1	.025	2600	30	28	7.28	95	14/A/10E
2.7	18.1	.05	1400	60	60	8.40	85	17/A/17
2.7	18.1	.05	2500	58	48	12.00	87.5	31/A/17
2.7	18.1	.05	3400	50	40	13.60	90	12/A/17
2.7	18.1	.05	3100	46	32	9.92	92.5	40/A/12E
2.7	18.1	.05	3000	40	30	9.90	95	9/A/12E
3.0	30.5	.05	250	52	52	1.30	87.5	73/A/19
3.0	30.5	.05	3100	52	52	16.12	90	64/A/19
3.0	30.5	.05	3150	48	41	12.80	92.5	51/A/19
3.0	30.5	.05	2700	39	38	10.26	95	36/A/19
3.6	30.5	.075	220	56	40	0.88	85	25/A/19
3.6	30.5	.075	380	53	44	1.672	87.5	21/A/19
3.6	30.5	.075	700	44	36	2.52	90	11/A/19
3.6	30.5	.075	2600	48	40	10.40	92.5	21/A/18
3.6	30.5	.075	3100	40	28	8.68	95	11/A/18

V^* = Voltage corresponding to I_{max}

$P^* = V^* I_{max}$

at 85% helium and the trend observed as the He% was decreased from 95% indicated that an extensive search at lower helium percentages would be both uninteresting and futile. Brief excursions into the region of very low helium percentages throughout the entire experimentation time indicated that the trend noted in the data was an accurate one and nothing had been lost by not pursuing an intensive search further. Helium percentages above 95% were not looked at because of the small amount of CO_2, the active medium, in such a mixture.

This discussion is not meant to infer that any other laser configurations or even any other double discharge lasers configured similarly to this one are constrained to the same narrow operating region. As pointed out earlier, many laser configurations rely on different mechanisms for their operation and are constrained to operate at different (shorter) rise times. Interestingly enough, even the laser used by Pan [3], a very similar configuration to that used here, operated best with gas mixtures containing much lower concentrations of helium (60%-80%) and a shorter optimum rise time (on the order of 2 μsec).

Several trends can be noted from the data presented in Figures 12 and 13. The most obvious effect is the rapid decrease seen in the maximum attainable current as the helium percentage decreases. This effect is most pronounced at the longer rise times, i.e. 3 μsec and 3.6 μsec. At τ_r = 3 μsec the current decreases from 3100 amperes at 90%

He to 250 amperes at 87.5% He. At τ_r = 3.6 μsec the current decreases from 2600 amperes at 92.5% He to 700 amperes at 90% He. A marked change in discharge appearance accompanied this precipitous decrease in I_{max}. The glow discharge yielding the high currents, in general, was bright and appeared to be very uniform throughout the entire discharge volume. The discharge yielding the lower currents appeared to be very stratified, i.e., composed of many fingers. It was interesting to note that the low current discharges at τ_r = 3.6 μsec and 3.0 μsec appeared to be very similar to the discharges observed when the trigger was inactive. The discharges were weak and the streamers observed grew from the anode. They appeared to follow the "classical" electric field lines expected at the edges for finite flat electrode geometry, i.e., they tended to be bowed outward at the edges of the electrodes. The fingers were not observed at any areas of the electrodes except near the edges. This behavior was observed to accompany the low current discharges only for the longer rise time circuits. The low current discharges observed with the shorter rise time circuits had a stratified appearance but the fingers were not confined to the edges of the electrodes and were not bowed outward. It therefore appears that the mechanisms limiting the discharge operation at low helium percentages for short and long rise times are different. We are not prepared to speculate about the precise limiting mechanism at work in either case.

The values of power plotted on Figure 14 are those values of power obtained at the times corresponding to the maximum current plotted in Figure 12. It can be seen that at almost all rise times given P_{max} falls off at 95% He when compared to 92.5% He and to 90% He, whereas I_{max} is consistently high at 95% He. This occurs because at higher helium percentages the plasma resistance during the discharge is lower since the electrons reach a higher T_e[2]. So, for similar currents the voltage across the discharge is appreciably lower at 95% He than at 92.5% or 90% He.

It can then be seen from the figures that while the regime for glow discharge operation is narrow, the optimum operating region is only a small part of that. The quality of operation decreases rapidly away from this optimum region. With respect to power the optimum operating condition with C_m = .167 μf was found to be:

$$\tau_r = 3 \text{ μsec}$$

$$\text{He\%} = 90\%$$

This condition yielded a power of 161.2 MW with an associated current of 3100 amperes (64/A/19).

B. DEPENDENCE OF I_{max} AND V_{max} ON V_o

When operating in a regime in which V_o, the voltage applied, was well above the glow discharge threshold, the trend of operation observed was very interesting. The applicable data (V_o, V_{max} and I_{max}) from two series of shots is presented in Tables III and IV and plotted in

TABLE III

V_{max} and I_{max} vs V_o (1-5/A/17)

He% = 90% R = 16.8 ohms L^* = 0 C_m = .167 μf

L = 18.1 μh C_t = .004 μf

C_2 = .05 μh

V_o(kV)	V_{max}(kV)	I_{max}(amperes)
48	50	800
51	52	1050
54	50	1350
57	52	1650
60	54	1950

TABLE IV

V_{max} and I_{max} vs V_o (5-9/A/10)

He% = 87.5% R = 7.6 ohms L^* = 2.7 μh C_m = .167 μf

L = 18.1μh C_t = .004 μf

C_2 = .025 μf

V_o(kV)	V_{max}(kV)	I_{max}(amperes)
48	50	250
51	52	550
54	52	850
57	54	1050
60	54	1100

Figures 15 and 16. The error bars used for V_{max} are ±2 kV and represent the accuracy that can be expected in taking the voltage data from the scope traces. It was felt that the current values, I_{max}, could be read within ±50 amperes. Because of scaling limitations, the error bars aren't shown on the figures. It can be seen that in Figure 16 a 25% variation in V_o results in only about an 8% variation in V_{max} but a variation in I_{max} which is slightly greater than 145%. Similarly, Figure 15 shows an 8% variation in V_{max} but a 45% variation in I_{max} corresponding to a 25% increase in V_o. These were not isolated instances of this behavior. The same behavior was observed throughout the course of experimentation and appeared to be dependent only on the fact that the region of operation was one in which favorable operation could be achieved well above the glow discharge threshold. Operating in regions near the glow discharge threshold yielded results in which V_{max} increased nearly linearly with V_o.

C. VARIATION OF DISCHARGE RESISTANCE AS ARCING IS APPROACHED

The data presented above has some interesting implications for discharge conditions which lead to arcing. It was found that for a given condition if all other parameters were held constant while V_o was increased, eventually arcing would occur. However, as was pointed out, as V_o was increased, V_{max} remained essentially constant. Thus, as far as the discharge was concerned, the maximum applied voltage

had not changed. An interesting question arises then--in the production of an arcing condition, what threshold has been exceeded? Clearly, since V_{max} essentially remained unchanged, the arcing threshold is not a simple voltage threshold.

In order to investigate the change in the discharge conditions accompanying the approach of the arcing threshold, the graphs presented in Figures 17 through 19 were plotted (Tables V through VIII). The parameters common to all of the shots were:

C_m = .167 μf

C_2 = .05 μf

C_t = .004 μf

L = 18.1 μh

R = 35.5 ohms

He%= 90%

τ_r = 2.7 μsec

The voltage was varied on successive shots from V_o= 51 kV to V_o= 58.5 kV. Arcing occurred at V_o= 58.5 kV.

Careful investigation of the graphs shows them to be similar in shape and to have minimum values of approximately the same magnitude right up until the time at which arcing occurred. In comparing these curves, it must be noticed that different scales were used on each graph. There does not appear to be any dramatic change in the $\Omega(t)$ curve for an arcing condition, as compared to a non-arcing condition, until the actual arc occurs.

TABLE V

Ω(t): Arcing Trend Investigation (10/A/17)

V_o = 51 kV

Time (μsec)	Current(amperes)	Voltage(kV)	V/I= Ω (ohms)
1.4	0	40	∞
1.6	100	48	480.0
2.0	1000	52	52.0
2.4	2200	49	22.3
2.6	2600	46	17.7
2.7	2700	45	16.6
2.8	2600	44	16.9
3.0	2300	42	18.3
3.4	1400	32	22.8
3.8	400	22	55.0
4.0	100	20	200.0
4.2	0	12	∞

TABLE VI

Ω(t): Arcing Trend Investigation (11/A/17)

V_o = 54 kV

Time (μsec)	Current(amperes)	Voltage (kV)	V/I= Ω (ohms)
1.4	0	42	∞
1.6	200	54	270.0
2.0	1000	52	52.0
2.2	2000	49	24.5
2.6	2900	44	15.7
2.7	3000	42	14.0
2.8	2900	42	14.9
3.2	2000	36	18.0
3.5	1000	26	26.0
4.0	200	12	60.0
4.2	0	9	∞

TABLE VII

Ω(t): Arcing Trend Investigation (12/A/17)

V_o = 57 kV

Time (μsec)	Current(amperes)	Voltage(kV)	V/I= Ω (ohms)
1.4	0	40	∞
1.6	400	48	120.0
1.8	500	50	100.0
2.0	1400	52	37.1
2.4	3000	50	16.6
2.6	3300	46	13.9
2.7	3400	44	12.9
3.0	2700	40	14.8
3.4	1500	28	18.6
3.8	400	18	45.0
4.0	200	14	70.0
4.4	0	9	∞

TABLE VIII

Ω(t): Arcing Trend Investigation (13/A/17)

V_o = 58.5 kV

Time (μsec)	Current(amperes)	Voltage(kV)	V/I= Ω (ohms)
1.4	0	20	∞
1.6	500	28	56.0
2.0	2000	45	24.5
2.4	3300	54	16.4
2.6	3600	52	14.4
2.7	3700	49	13.2
2.8	3500	48	13.7
3.0	2900	46	15.9
3.6	1200	43	35.8
4.0	600	30	50.0
4.2	0	27	∞
4.8	0	5	∞
5.0	500	8	16.0
5.2	900	8	8.9
6.0	1800	8	4.4
6.2	1700	12	7.0
6.4	1400	10	7.1
6.8	600	8	13.3
7.0	200	8	40.0

So again, the question can be raised--"How does the plasma know that V_o has been changed?" As can be seen in the tables, I_{max} exhibited a strong dependence on V_o. In addition, the tables show that at the time of I_{max}, V is greater under the arcing condition than under the non-arcing conditions.

It therefore appears that there are two quantities of interest to be considered in the investigation of the conditions which limit the operation of the double discharge in high current regimes. These quantities are I_{max} and the relationship of I(t) and V(t). It can be seen from the tables and figures presented that it was this latter quantity which kept $\Omega(t)_{min}$ relatively unchanged as I_{max} increased with increasing V_o.

D. DEPENDENCE OF V_{max} ON He%

The results of the investigation of the dependence of V_{max} on the helium percentage present in the gas mixture are presented in Figure 20. Briefly, it was found that under conditions which yield a strong discharge (I_{max} > 1000 amperes),the maximum voltage across the discharge, V_{max}, is strongly dependent on the He% of the gas mixture. At the same time, V_{max} appears to be relatively independent of τ_r, R, L^* and V_o. As Figure 20 clearly shows, in general V_{max} tended to decrease with increasing helium percentage. This dependence is believed to be due to an increase in the discharge plasma conductivity with increasing helium percentage.

This investigation was carried out with a 6 cm gap. The behavior, however, is consistent with that observed earlier with a 2 cm gap [2].

This relationship was found to hold except when a reduction in helium percentage resulted in a severe degradation of the discharge. The result of discharge degradation can be seen on the curve for τ_r = 3 μsec in Figure 20. The reduction from 90% He to 87.5% He was accompanied by a decrease in I_{max} from 3100 amperes to 250 amperes, a decrease which represents a severe degradation of the discharge. With 90% He in the gas mixture, a bright, uniform plasma was produced in the gap; whereas, with the 87.5% He mixture the discharge consisted of many weak fingers concentrated around the electrode edge. No bright uniform plasma was produced. This abrupt change in the discharge plasma properties is reflected in the break in the curve (τ_r= 3 μsec) in Figure 20.

The reduction in V_{max} for the "weak discharge condition" can be explained in the following way. In the weak discharge, the plasma conductivity cannot "control" the gap voltage. Under these conditions, it is found that $V_{max} \gtrsim V_o$. In addition, arc formation begins at relatively low values of V_o under the weak discharge conditions. This is probably due to the absence of the strong preionization with its tendency to even out the electric field concentrations at the electrode edges.

E. CALCULATIONS

The dependence of V_{max} on He% pointed out in the previous section leads on to speculate that the equilibrium condition of the plasma is dependent on the helium percentage of the gas mixture rather than on V_o. The equilibrium condition of the plasma is characterized by the quantity $(E/p)_{max}$ where $E = V_{max}/d$ is the electric field (V/cm) in the gap and p is the pressure (torr) in the gap. Table IX lists some characteristic values of $(E/p)_{max}$ and the corresponding helium percentages.

TABLE IX
Calculated Values of $(E/p)_{max}$

He%	$(E/p)_{max}$ (V/cm·torr)	Shot
95%	8.8	(20/A/17)
90%	11.4	(7/A/17)
85%	12.9	(17/A/17)

It is interesting to note that these $(E/p)_{max}$ values are generally lower than the value of 14 V/cm·torr generally thought of as the optimum value for such double discharge systems.

The question may arise, "How valid is the parameter $(E/p)_{max}$?" The following brief calculations were performed in an effort to determine whether or not $(E/p)_{max}$ is a meaningful parameter.

At 95% He, (20/A/17):

$$(E/p)_{max} = \frac{V_{max}}{pd} = \frac{40 \times 10^3}{(760)(6)}$$

$$= 8.8 \text{ V/cm·torr}$$

The discharge resistance of the gap is given by:

$$\Omega = V/I_{max} = 3.4 \times 10^4/2.6 \times 10^3$$

$$= 13 \text{ ohms}$$

where 3.4×10^4 V is the voltage across the gap at the time corresponding to I_{max}. Then the resistivity is given by:

$$\eta = \frac{\Omega A}{d} = \frac{(13)(.09)}{(.06)} = 19.7 \text{ ohm·m}$$

Taking into account electron collision cross sections with each of the gas constituents, the effective rate of momentum transfer collisions is given by:

$$\nu_{eff} = \{[.95(4.3) + 0.25(9) + .025(11.5)] \times 10^{-8}\} 2.5 \times 10^{19}$$

$$= 1.1 \times 10^{12} \text{ sec}^{-1}$$

The calculation for ν_{eff} is explained thoroughly in Ref.[2]. The electron density is given by:

$$n_e = \frac{m_e \nu_{eff}}{ne^2}$$

where m_e is the electron mass and e is the electron charge. Substituting in the values for m_e and e yields:

$$n_e = 2 \times 10^{12} \text{cm}^{-3}$$

Now, $I = J \cdot A$

$$J_{max} = \frac{I_{max}}{A} = \frac{2.6 \times 10^3}{.09} = .29 \times 10^5 \ \frac{amps}{m^2}$$

But, $J = n_e e V_D$

V_D can therefore be calculated from:

$$V_D = \frac{J_{max}}{n_e e}$$

$$= \frac{.29 \times 10^5}{(2 \times 10^{12})(1.6 \times 10^{-19})}$$

$$= 9.1 \times 10^6 \ \frac{cm}{sec}$$

These results are encouraging. Since the value calculated for n_e is typical of the electron densities expected for such systems and V_D agrees quite well with the value expected in 100% He at E/p=8.8, it appears that $(E/p)_{max}$ may be a useful parameter for characterizing such double discharge configurations.

F. DEPENDENCE OF DISCHARGE RESISTANCE ON He%

The data presented in Tables X through XIV is plotted in Figures 21 through 23. The parameters common to all of the shots used to collect the data were:

$C_m = .167$ μf

$L = 18.1$ μh

$C_2 = .05$ μf

$C_t = .004$ μf

$L^* = 0$

It must be noted that although the time scales for the three plots are the same, the scale of the discharge resistance is different in each case. Nevertheless, careful study of the tables and figures shows several interesting trends. First, the minimum value of plasma resistance during the discharge increases with decreasing helium percentage in the gas mixture. As an example, the minimum value attained with the 95% He mixture was 12.3 ohms while the resistance for the 90% He mixture got only as low as 16.92 ohms and the 85% He mixture had a minimum resistance of 26.66 ohms.

Secondly, it can be seen that in addition to the higher helium percentage mixtures having a lower minimum value, the discharge resistance stays low for a longer period of time.

These two trends comprise what was referred to as the "window condition" in Ref. 2. It was discussed in great detail there.

It should be noted that these two trends can be observed through direct comparison of any two conditions except the 87.5% He and the 85% He conditions. We cannot at present explain this discrepancy.

TABLE X

Ω vs t: Variation with He% (11/A/12E)

He% = 95% V_o = 48 kV R = 27.1 ohms

Time (μsec)	Current(amperes)	Voltage(kV)	V/I= Ω(ohms)
1.4	0	28	∞
2.0	1700	38	22.4
2.2	2000	38	19.0
2.4	2600	36	13.8
2.5	2750	36	13.1
2.8	2600	32	12.3
3.0	2000	28	14.0
3.4	1000	21	21.0
3.6	600	16	26.6
3.8	200	8	40.0
4.0	0	6	∞

TABLE XI

Ω vs t: Variation with He% (33/A/12E)

He% = 92.5% V_o = 54 kV R = 27.1 ohms

Time (μsec)	Current(amperes)	Voltage(kV)	V/I= Ω(ohms)
1.4	0	36	∞
1.6	300	40	133.0
1.8	600	48	80.0
2.0	1400	46	32.8
2.2	2200	43	19.5
2.4	2600	41	15.7
2.6	2850	40	14.0
2.7	2900	40	13.7
2.8	2850	39	13.6
3.0	2300	36	15.6
3.4	1200	18	15.0
3.8	300	14	46.6
4.0	0	10	∞

TABLE XII

Ω vs t: Variation with He% (7/A/17)

He% = 90% V_o = 54 kV R = 25.8 ohms

Time (μsec)	Current(amperes)	Voltage(kV)	V/I= Ω(ohms)
1.6	0	43	∞
1.8	200	52	260.0
2.0	900	50	55.5
2.2	1600	48	30.0
2.3	2000	48	24.0
2.6	2400	45	18.8
2.7	2600	44	16.9
2.8	2500	44	17.6
3.0	2100	40	19.0
3.5	1000	28	28.0
4.0	100	14	140.0
4.2	0	8	∞

TABLE XIII

Ω vs t: Variation with He% (26/A/17)

He% = 87.5% V_o = 54 kV R = 25.4 ohms

Time (μsec)	Current(amperes)	Voltage(kV)	V/I= Ω(ohms)
1.6	0	56	∞
1.8	100	58	580.0
2.0	300	60	200.0
2.6	1300	56	43.1
2.7	1500	54	36.0
2.8	1400	53	37.8
3.0	1200	50	41.7
3.5	600	32	53.3
4.0	100	20	200.0
4.2	0	16	∞

TABLE XIV

Ω vs t: Variation with He% (17/A/17)

He% = 85% V_o = 54 kV R = 25.5 ohms

Time (μsec)	Current(amperes)	Voltage(kV)	V/I= Ω(ohms)
1.7	0	52	∞
1.8	200	55	275.0
2.1	600	58	96.7
2.3	1300	56	43.1
2.5	1700	52	30.6
2.7	1800	48	26.7
2.9	1600	47	29.4
3.1	1200	44	36.7
3.5	700	30	42.8
3.9	300	14	46.7
4.1	0	10	∞

V. LASING

The purpose of this section is to report on the PRELIMINARY efforts to couple the EM energy at 10.6 microns out of the discharge. At this time lasing action has been achieved using a number of different mirror configurations for the optical cavity. Cavity lengths varying from 142 cm to 157 cm have been used.

The mirror configurations used to date have included a front mirror with partially transmitting characteristics as well as a number of polished copper mirrors with a hole at the center to provide the output coupling. The mirrors which have been used have had holes varying from 1/8" to 3/4" in diameter. Both a flat polished copper mirror and a concave polished copper mirror with a 1.5 m focal length have been successfully used as the back mirror. The specific mirror configurations used are indicated in Table XV.

Although many cavity configurations were looked at, only one discharge condition was used for the brief lasing study. The parameters of this condition were:

C_m = .367 μf

L = 30.5 μh

C_2 = .05 μf

R = 10.7 ohms

C_t = .004 μf

V_o = 60 kV

$$He\%/CO_2\%/N_2\% = 90\%/5\%/5\%$$

These parameters typically yielded:

$$I_{max} \simeq 3000 \text{ amperes}$$

$$V_{max} \simeq 56 \text{ kV}$$

$$\tau_r \simeq 2.9 - 3.0 \text{ } \mu\text{sec}$$

The energy coupled into the discharge was on the order of 175 joules/pulse.

The total EM energy output per pulse was measured using a Westinghouse Model RN-1 Laser Radiometer. This radiometer is designed to trap the beam energy from a laser in a bundle of fine, insulated copper wire which functions both as a calorimetric mass and as a bolometer element. The change in resistance of this wire element is proportional to the energy absorbed and is practically independent of the distribution of energy within the unit. The bolometer element is part of a conventional Wheatstone bridge circuit and the change of balance of the bridge is a measure of the beam energy. A photon drag detector with a 10 nsec rise time was used to measure instantaneous laser output power.

The maximum energy output per pulse that has been achieved at this time is 5 joules/pulse. A sketch of a laser output trace, having only 1.5 joule/pulse and peak power of only 1.3 MW, taken from the photon drag detector is shown in Figure 24. The discharge current trace is shown in the same figure. Note the following features of the output power pulse:

TABLE XV
Lasing Configurations

Front Mirror / Back Mirror	Copper-Flat	Copper Concave f=1.5 m
Germanium	X	X
Copper:		
1/8"		X
1/4"		X
1/2"		X
3/4"		X

"X" indicates a configuration with which lasing has been achieved.

1. It rises very rapidly after the discharge current reaches its peak value.
2. There are two distinct portions of the power pulse --an initial spike approximately .4μsec wide and a long tail greater than 2μsec long.

The shape of the power pulse and its timing relative to the current are similar to the results achieved by others with double discharge lasers. Its shape can be easily explained in terms of the energy level diagram in Figure 25. The initial spike is due to stimulated emission from CO_2 molecules which have undergone direct electron excitation to group II. These molecules fall to the lower laser level (group I) by stimulated emission until the populations of group II and group I levels are equal. Laser power output then falls off rapidly. After approximately .37μsec, the lower laser level (group I) depopulates and the population inversion is again rebuilt so that the rapid fall off in output power is halted. Finally, resonant transfer from the excited N_2 molecules (group III) continues to pump the CO_2 upper laser level for a time on the order of 2 to 3 μsec. This contributes to the long tail on the power pulse.

Since the energy stored in the Marx generator with V_o = 60 kV is approximately 660 joules, it can be immediately recognized that a 5 joule output represents an efficiency of only about .75%. It must be emphasized that this 5 joule output is representative of very preliminary efforts. It is expected that with further work and higher quality optics

an output energy of about 11 joules/pulse can be achieved. This estimate was arrived at in the following manner. In a similar double discharge laser built by Pan [3], a total energy of 341.25 joules was delivered to the discharge. His volume was 5.52 liters. Pan was then able to couple out 17 joules/liter of 10.6 micron radiation. This gives a coupling efficiency of 27.6%. Figure 26 shows the voltage and current traces for Pan's laser. The similarity between them and the voltage and current traces characteristic of the lasing condition presented here (Figure 27) is immediately evident. It is important to note that the gas mixture used by Pan contained only 60% He vice the 90% used in this configuration. Pan therefore had four times the active molecule (CO_2 and N_2) density as is present in this configuration. Since coupling efficiency (for similar discharge conditions) will depend only on resonant cavity losses and density of active molecules, we assume that with optimization of the resonant cavity we can achieve one-fourth the coupling efficiency of Pan. By these similarity arguments, since we put 175 joules into the discharge, we expect to be able to couple out 2.06 joules/liter at the present lasing condition by optimizing the resonant cavity. Our laser has a volume of 5.49 liters. This yields an expected pulse energy of about 11 joules.

By optimizing the resonant cavity and modifying the operating conditions to those which have previously coupled 285 joules into the discharge, it would be expected that about 18 joules/pulse could be coupled out.

At the present time, it appears that the limitations on output coupling are readily broken down into three categories. The first two limitations which will be discussed can be easily eliminated. The third limitation may be of a more permanent nature.

The Brewster angle mounts for the NaCl windows were designed for use with the 2 cm gap but are being used with the 6 cm gap configuration. This design does not properly align the windows with the gap. In fact, approximately 25% of the gap is obstructed by the lower portion of the window mount. This reduces the output energy by at least 25%. This problem should be very easy to overcome with only a slight modification or redesign of the existing mounts.

The work done thus far has shown that the optical components in use at the present time are inadequate. Under existing conditions, alignment of the optical cavity has proven to be a difficult procedure and a very temporary state of affairs. The current facilities for mounting the optical components make them too susceptible to vibration and it is very easy for the cavity to become misaligned. This problem could be alleviated through the use of better mirror mounts and an optical bench long enough on which to mount all of the mirrors and aligning equipment. The acquisition of a longer optical bench would also provide another advantage. At present the optical bench allows a maximum cavity length of only 157 cm. This length cavity does not allow utilization of the full discharge volume. A longer

bench would allow use of an unstable optical resonator configuration which would provide more complete utilization of the discharge volume. The preliminary work has also indicated the desirability of acquiring better mirrors. The scattering from the mirrors which can be readily observed during the aligning procedure demonstrates the irregularities of the surface. Further demonstration was provided by "microexplosions," small intense flashes on the face of the front mirror. The need for new mirrors is a financial limitation only.

The following problem, on the other hand, may represent a fundamental physical limitation of this system. As mentioned very briefly earlier in this section, the energy that could reasonably be expected to be coupled out from this system is down by a factor of four from that achieved by Pan [3] because he was able to operate at 60% He rather than 90% He. The limited regime of operation of this system was fully discussed earlier. Good discharge performance cannot be expected for gas mixtures much below 90% He. This restricts the density of active molecules to something on the order of 2.5×10^{18} cm^{-3} and may well represent a fundamental limitation to the performance of this system.

NOT TO SCALE
TOTAL LENGTH (LUCITE BASE): 40 in.

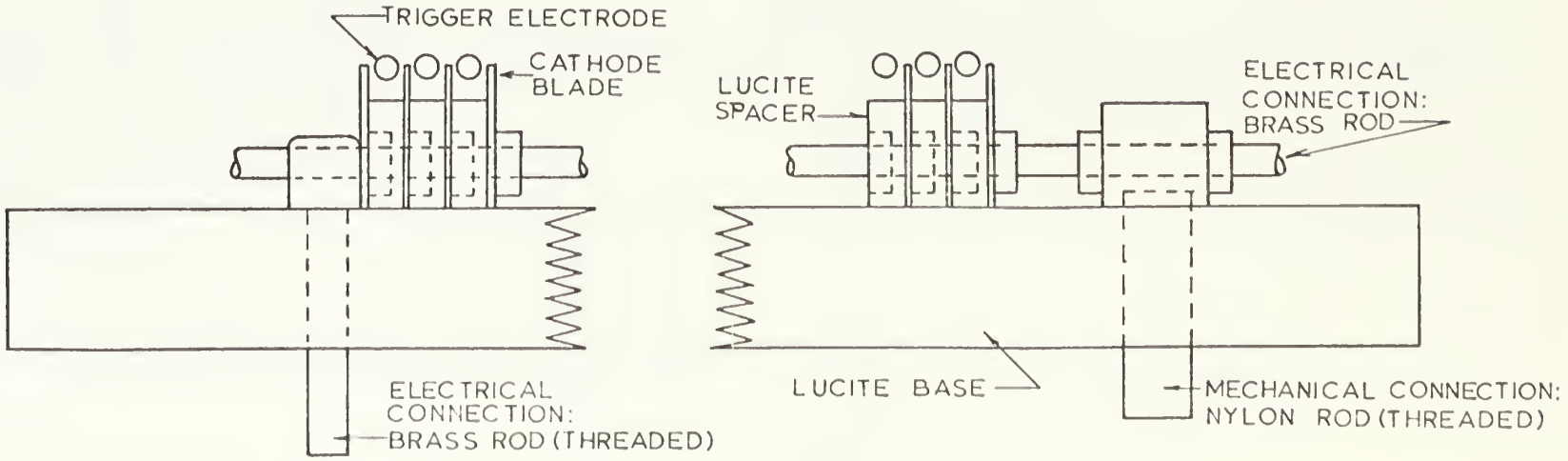

Figure 1

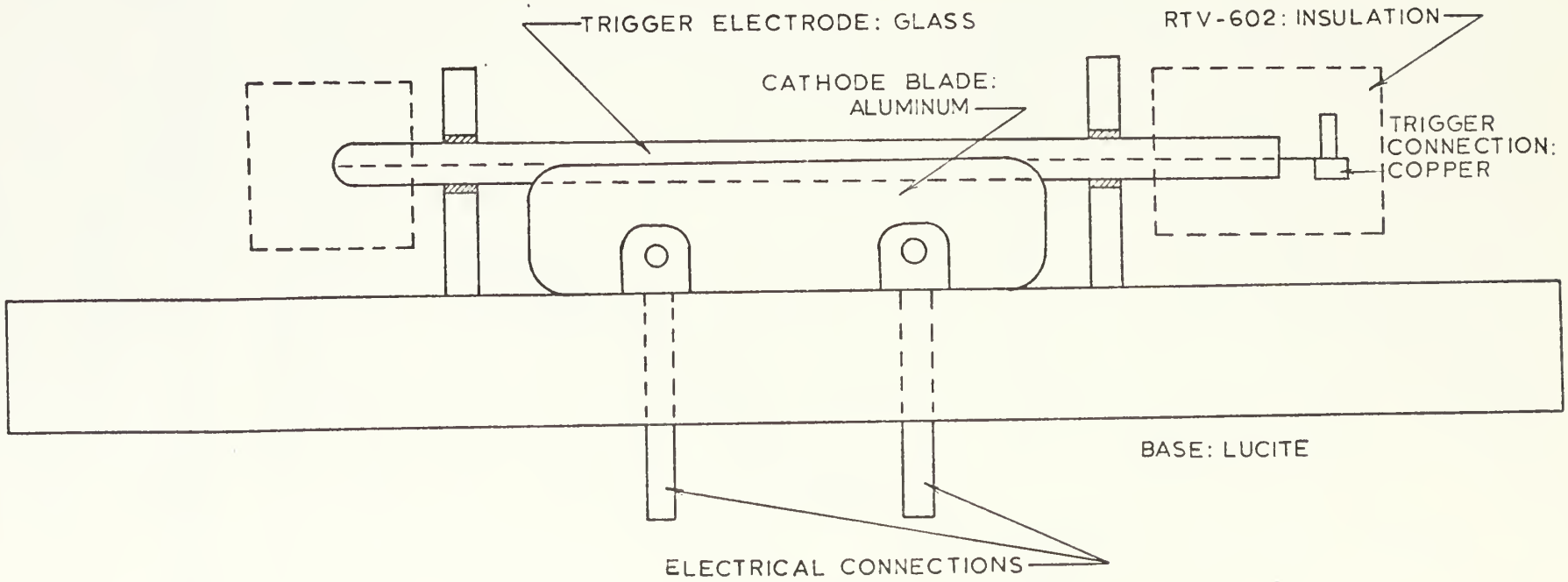
NOT TO SCALE
TOTAL WIDTH(LUCITE BASE): 12 in
TRIGGER ELECTRODE: GLASS
RTV-602: INSULATION
CATHODE BLADE: ALUMINUM
TRIGGER CONNECTION: COPPER
BASE: LUCITE
ELECTRICAL CONNECTIONS

Figure 2

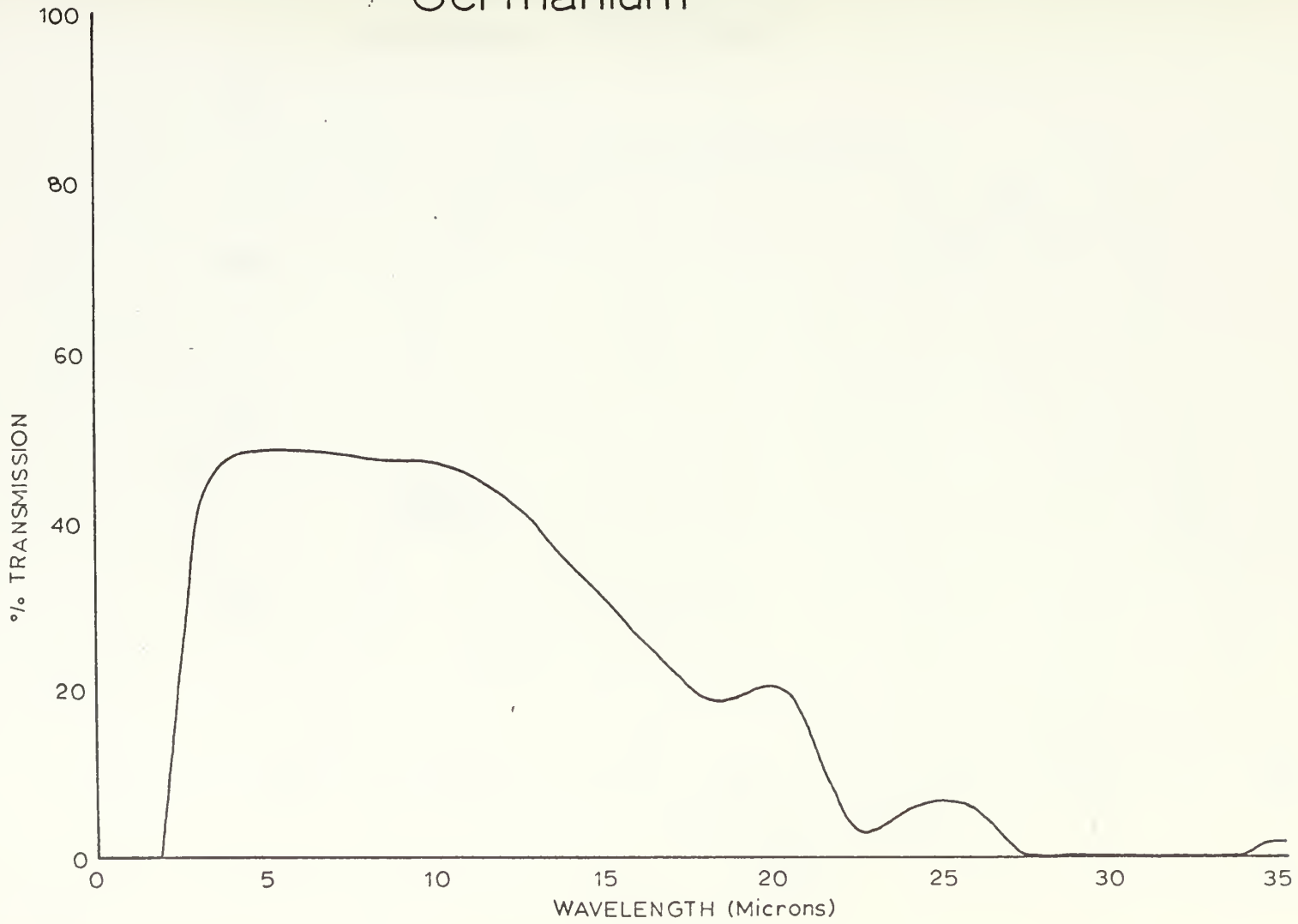
Germanium
100
80
60
40
20
0
% TRANSMISSION
0
5
10
15
20
25
30
35
WAVELENGTH (Microns)

Figure 3

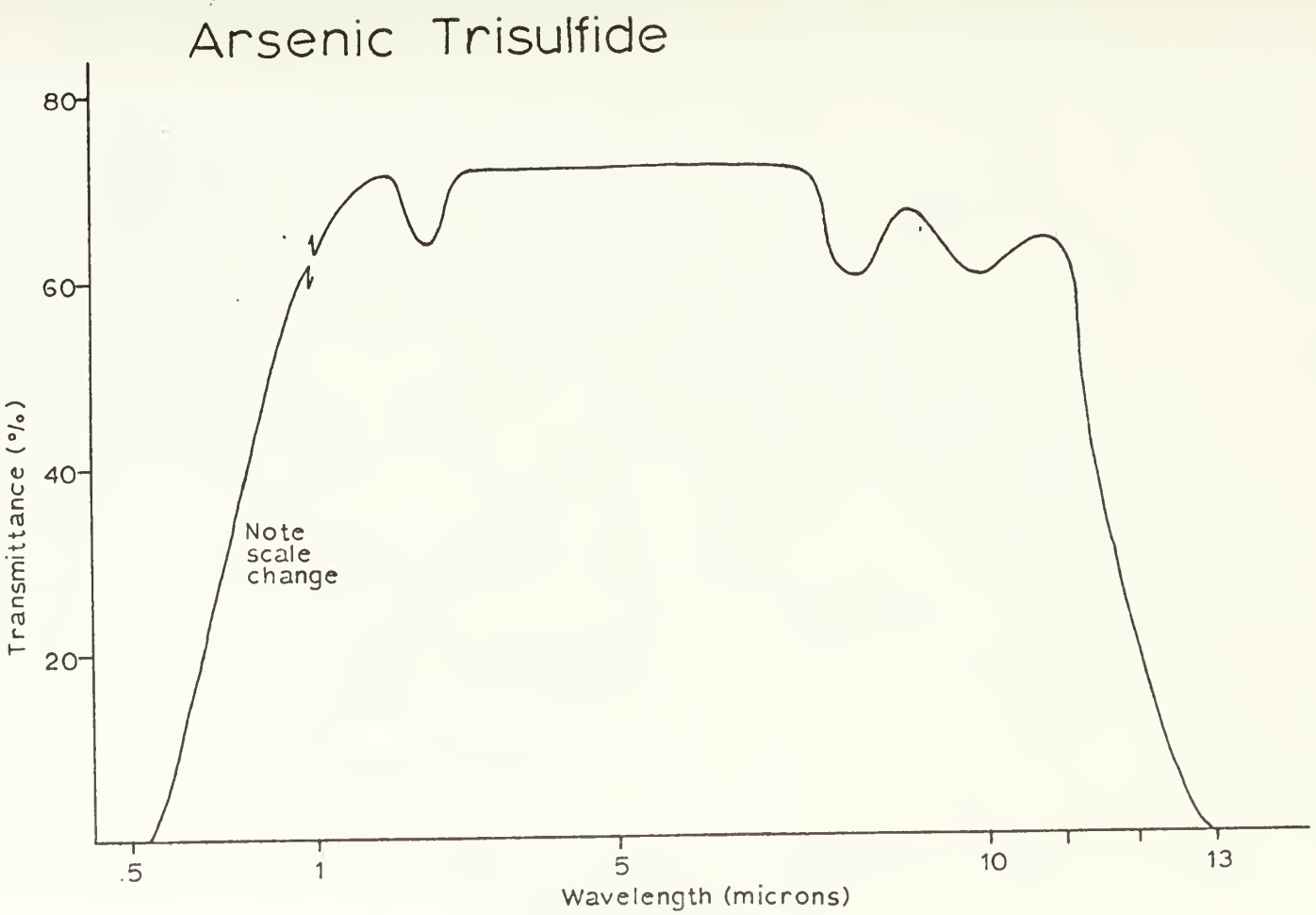
Arsenic Trisulfide
80
60
40
20
Transmittance (%)
Note
scale
change
.5
1
5
10
13
Wavelength (microns)

Figure 4

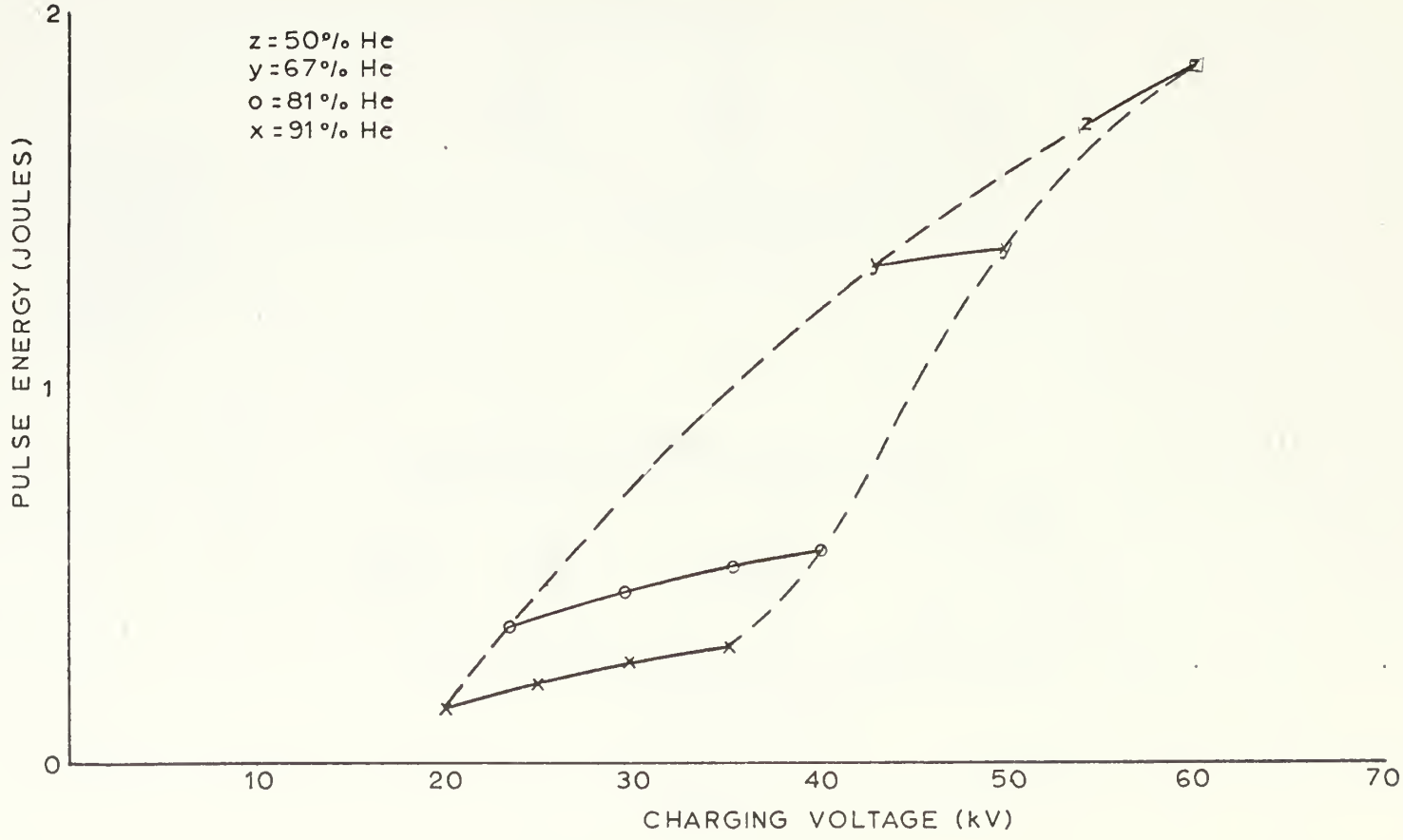
z = 50% He
y = 67% He
o = 81% He
x = 91% He
PULSE ENERGY (JOULES)
0
1
2
10
20
30
40
50
60
70
CHARGING VOLTAGE (kV)

Figure 5

R=5.8 ohms
C_m=.167 µf
C_2=.008µf
C_t=.008 µf
L_s=Stray
L=5.7µh

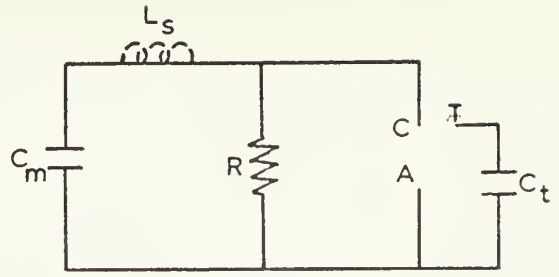

A. FAST CIRCUIT

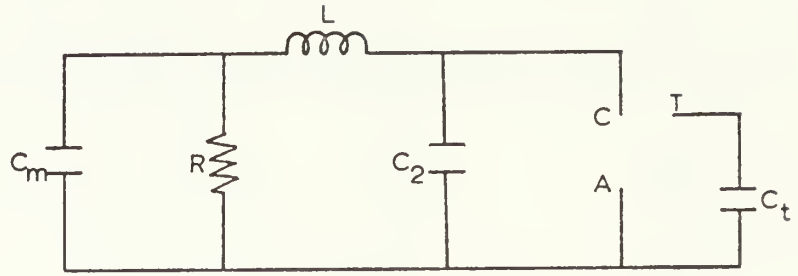

B. PAN'S CIRCUIT

Figure 6

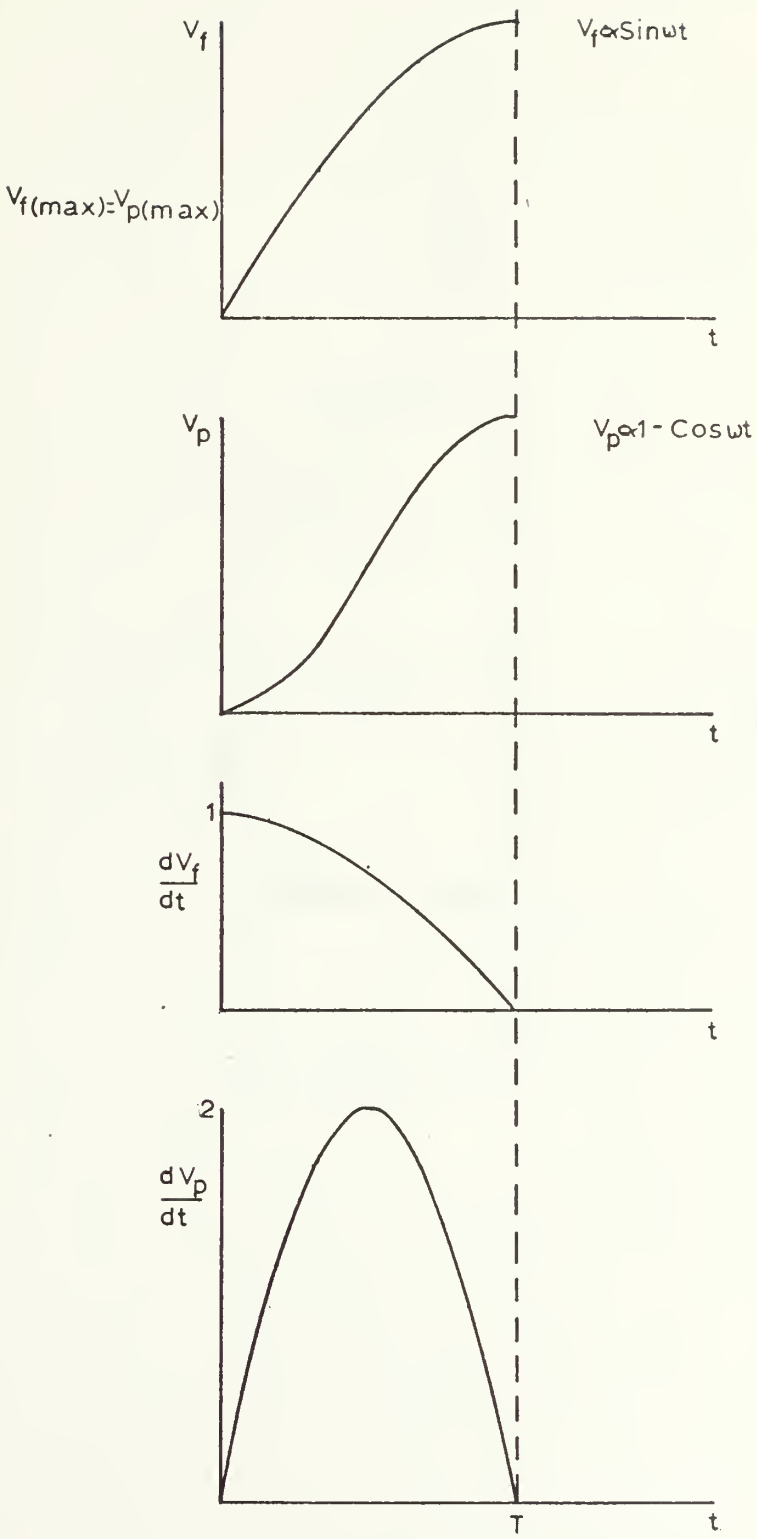
V_f
$V_f \propto \sin\omega t$
$V_{f(max)} = V_{p(max)}$
t
V_p
$V_p \propto 1 - \cos\omega t$
t
1
$\frac{dV_f}{dt}$
t
2
$\frac{dV_p}{dt}$
T
t

Figure 7

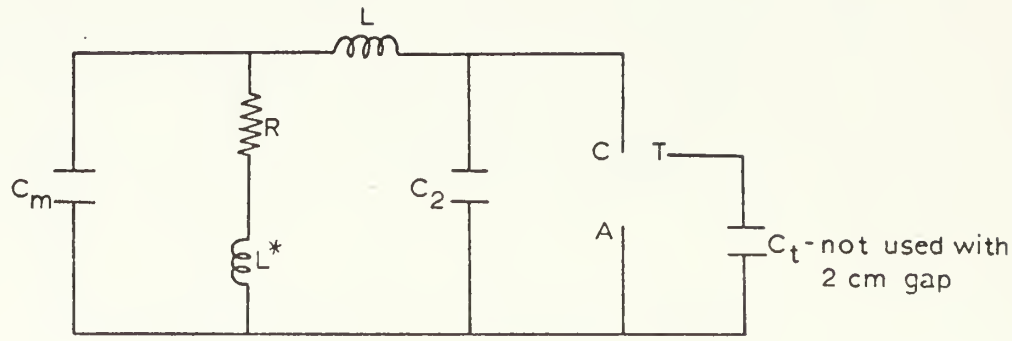

Figure 8

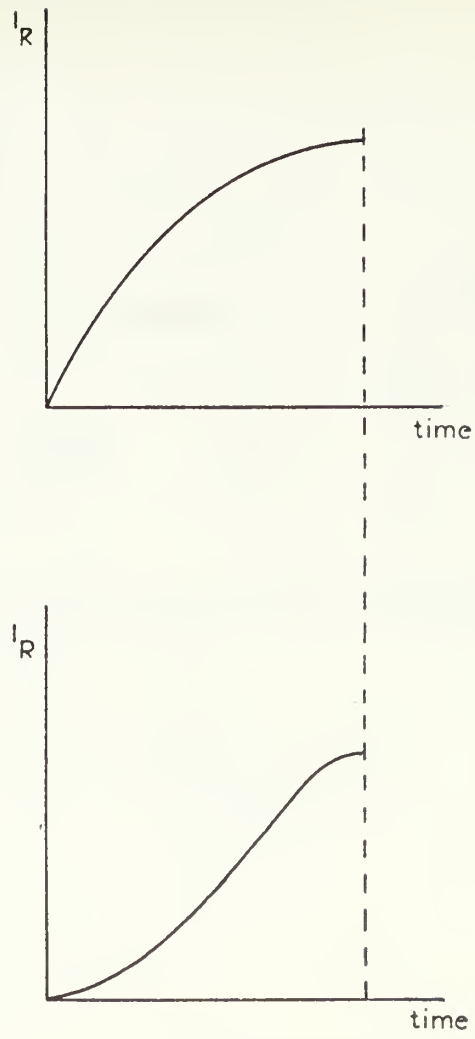

Figure 9

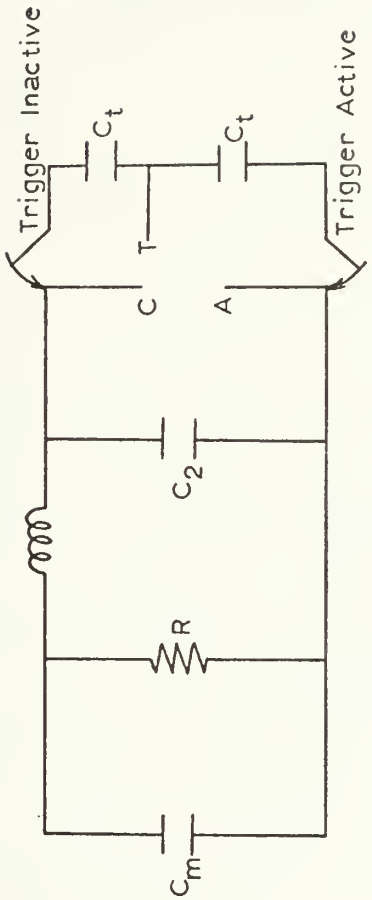

Figure 10

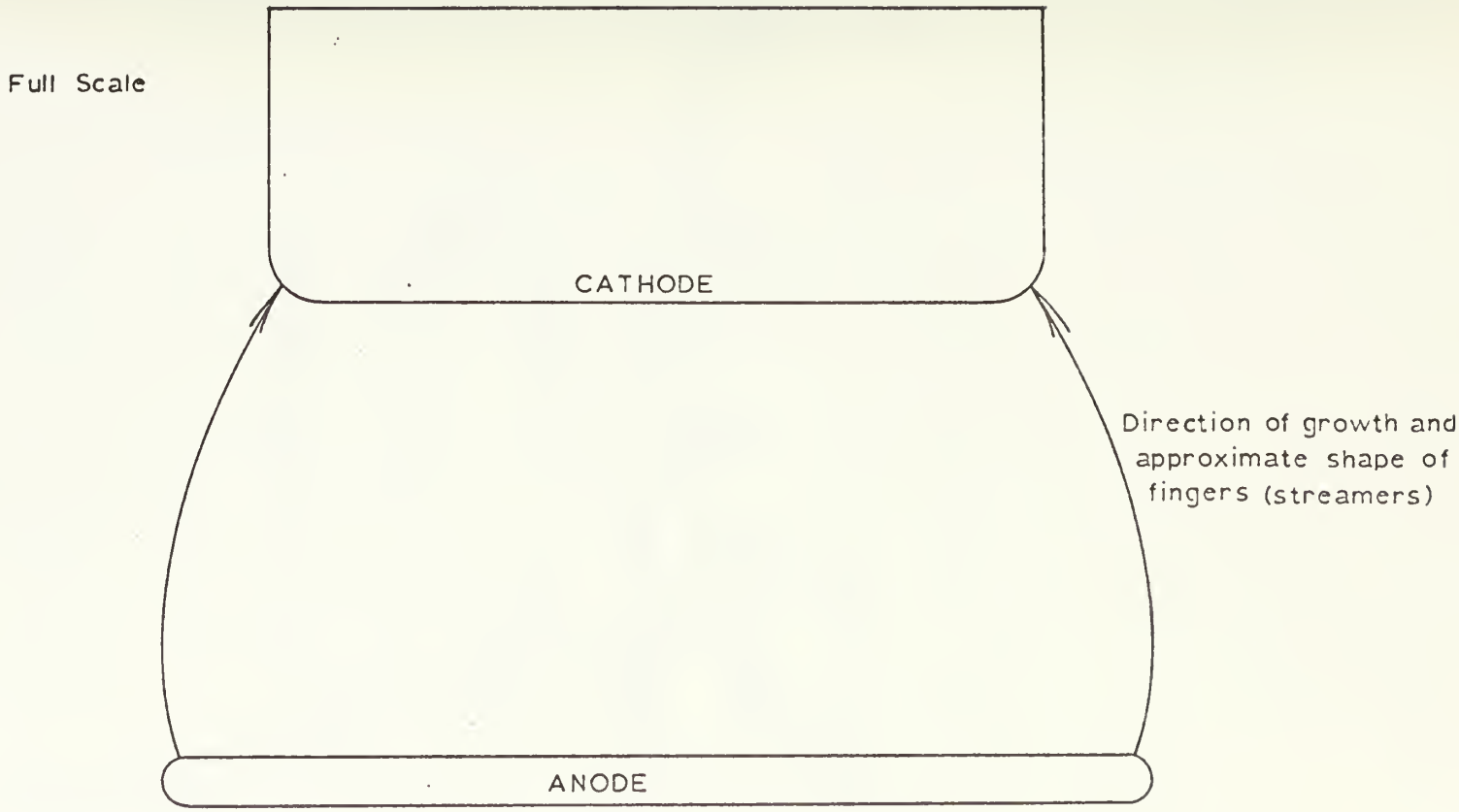
Full Scale
CATHODE
Direction of growth and approximate shape of fingers (streamers)
ANODE

Figure 11

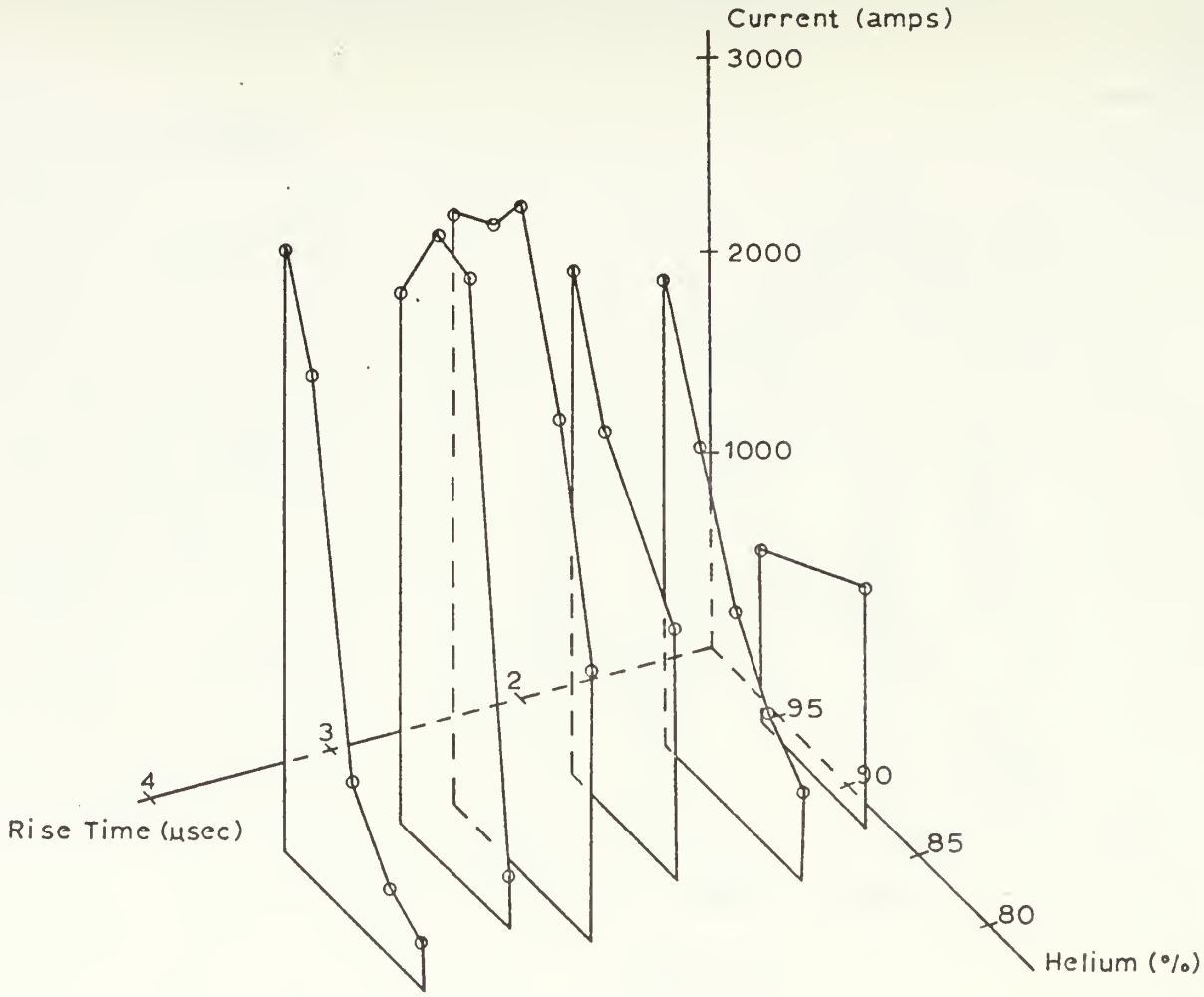
Current (amps)
3000
2000
1000
Rise Time (μsec)
4
3
2
95
90
85
80
Helium (%)

Figure 12

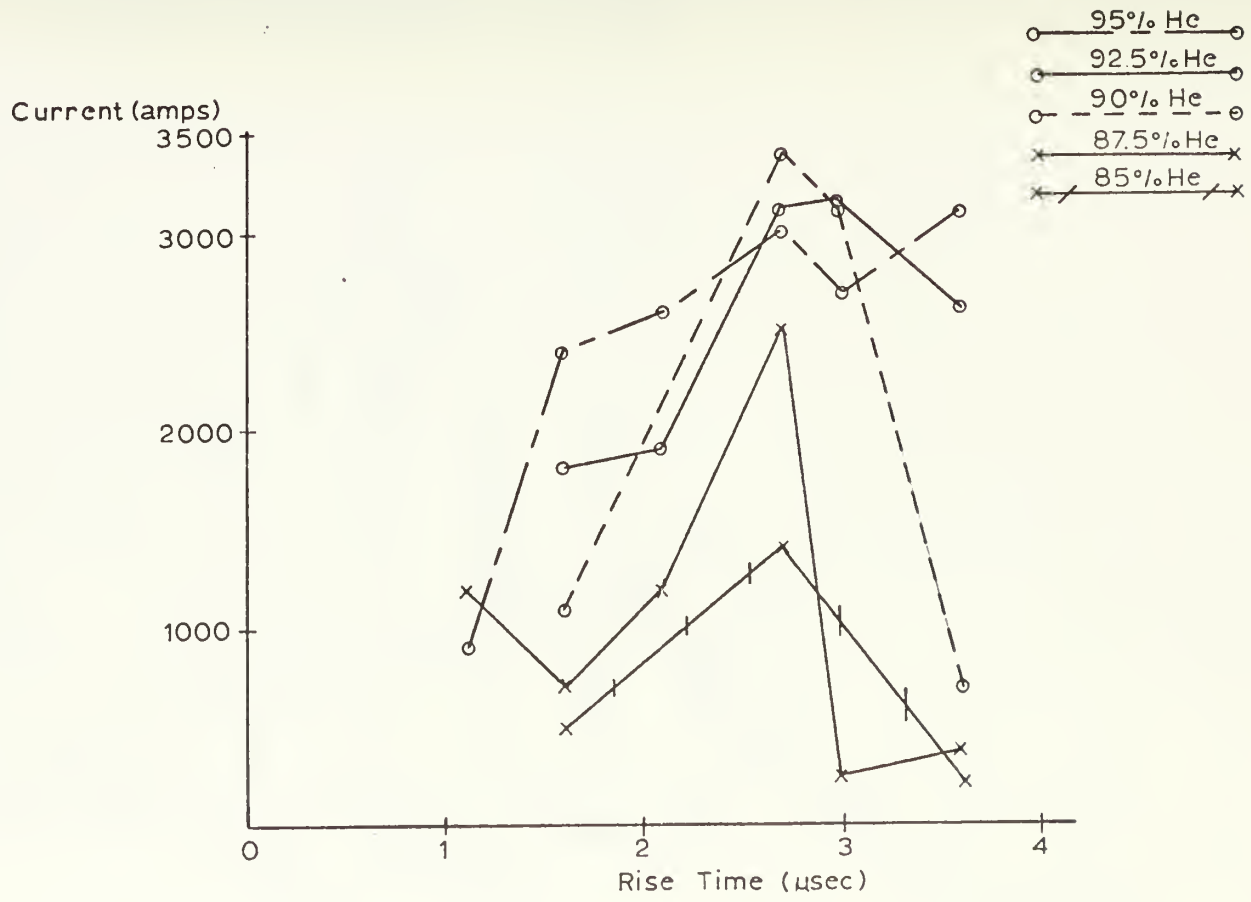
95% He
92.5% He
90% He
87.5% He
85% He
Current (amps)
3500
3000
2000
1000
0
1
2
3
4
Rise Time (μsec)

Figure 13

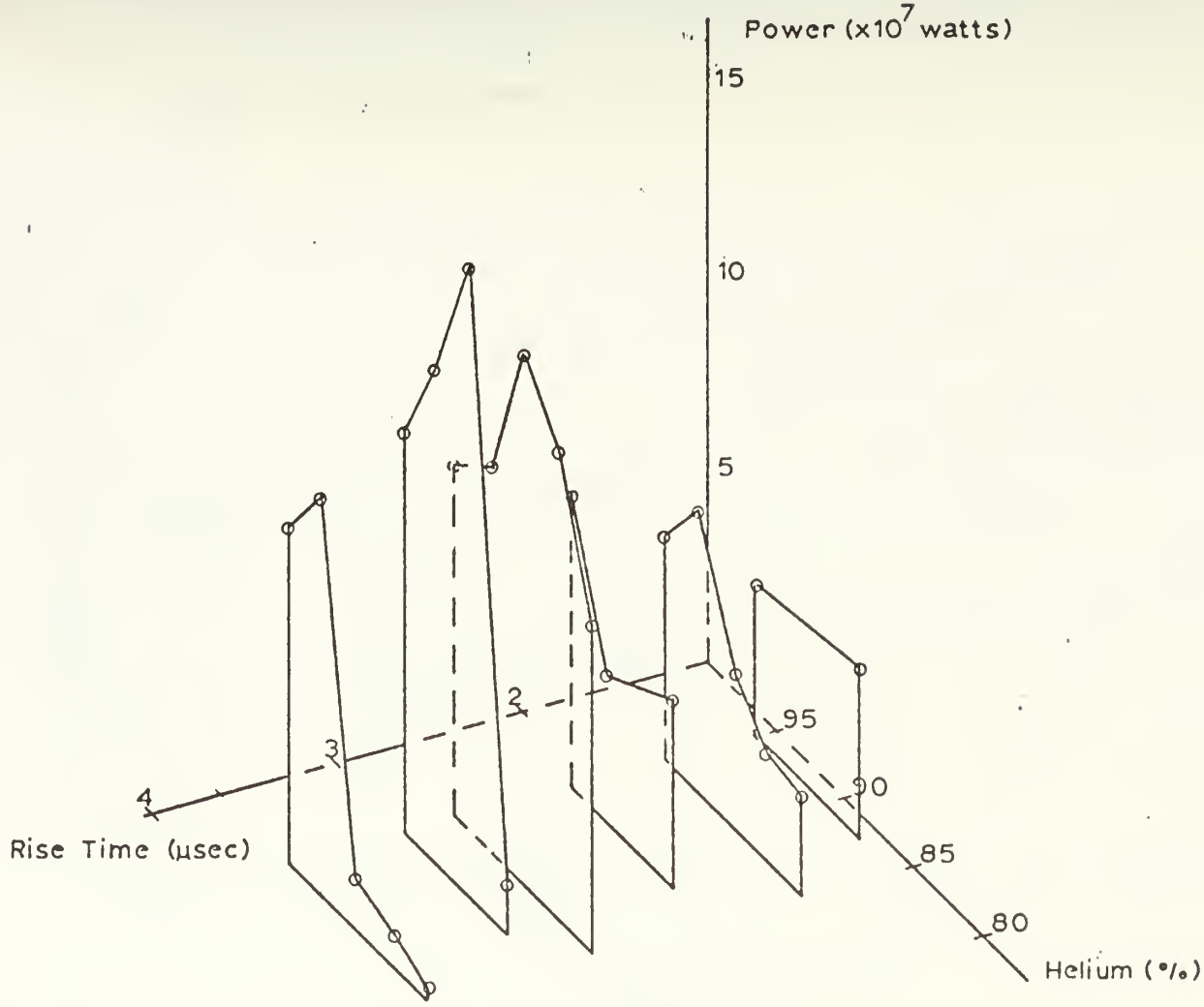

Figure 14

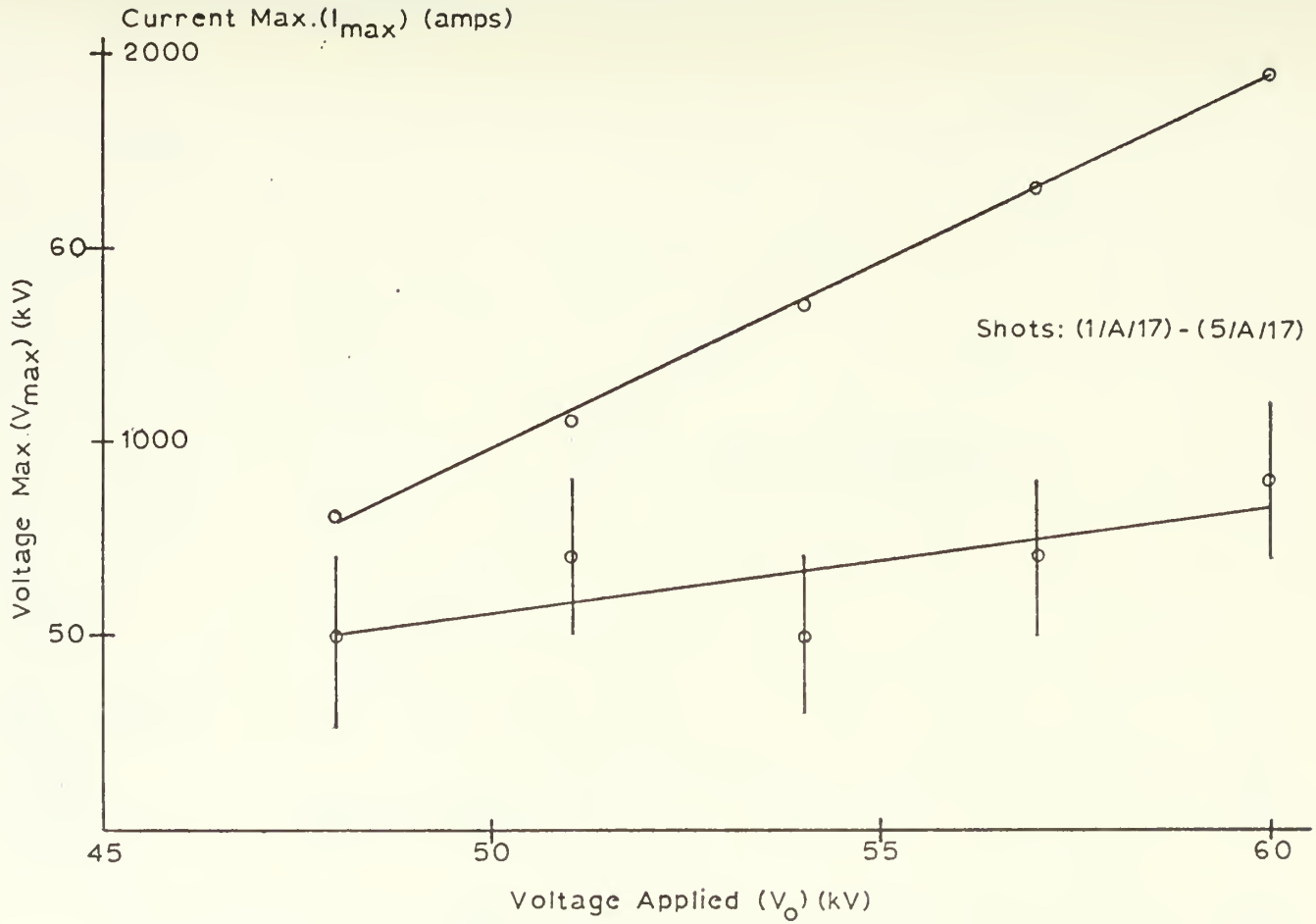
Current Max.(I_{max}) (amps)
2000
60
1000
50
Voltage Max.(V_{max}) (kV)
Shots: (1/A/17) - (5/A/17)
45
50
55
60
Voltage Applied (V_o) (kV)

Figure 15

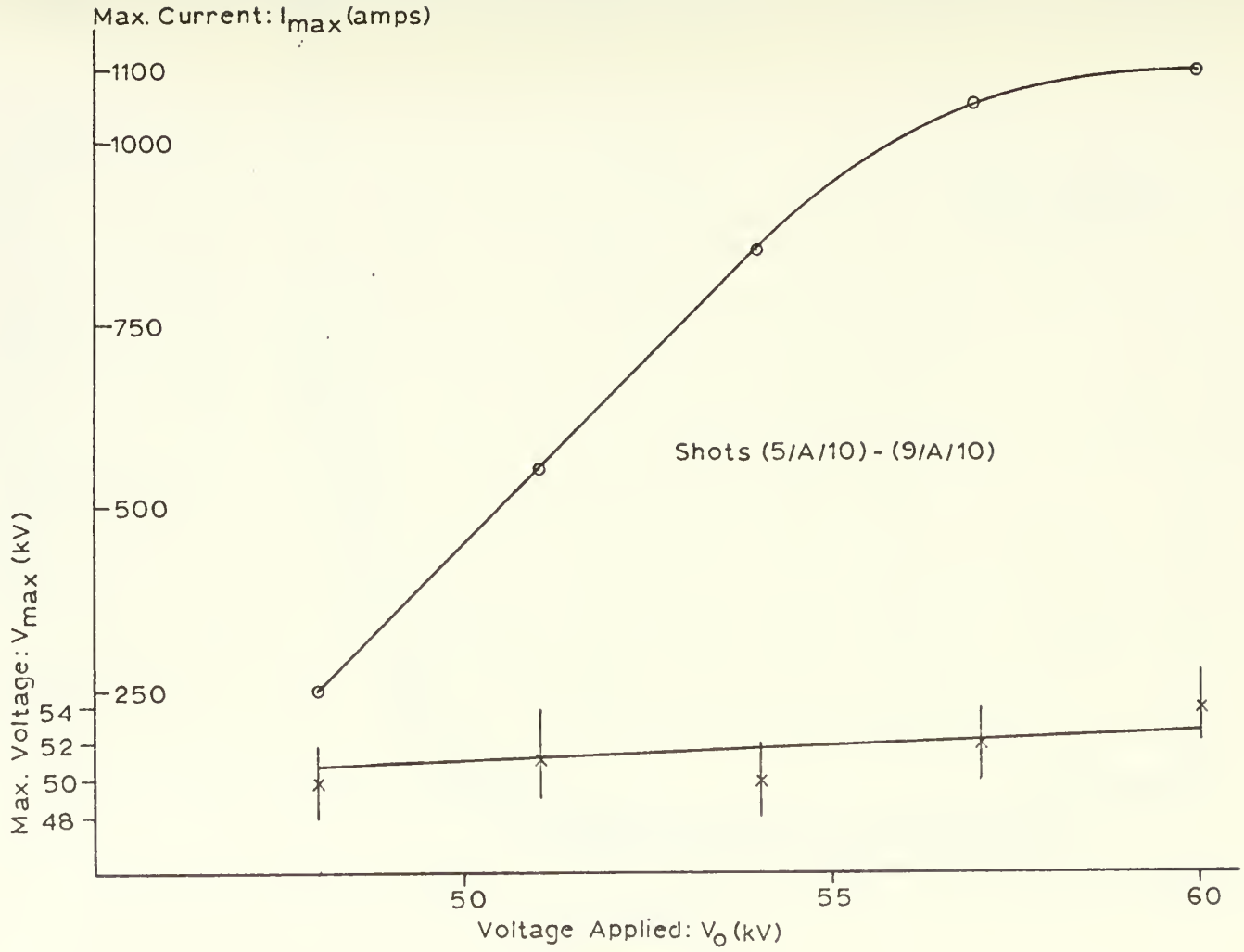
Max. Current: I_{max} (amps)
1100
1000
750
500
250
Shots (5/A/10) - (9/A/10)
Max. Voltage: V_{max} (kV)
54
52
50
48
50
55
60
Voltage Applied: V_o (kV)

Figure 16

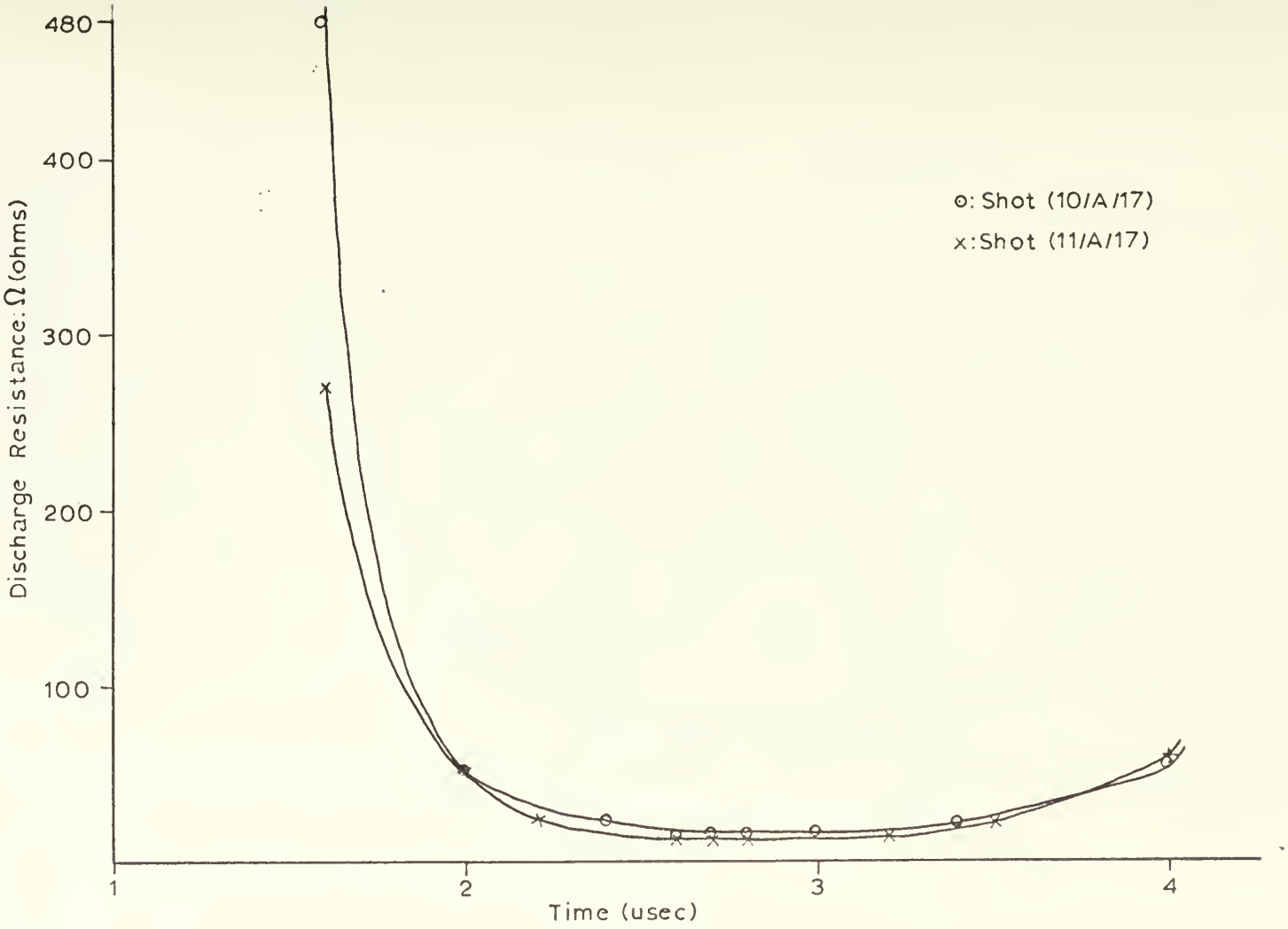
480
400
300
200
100
Discharge Resistance: Ω (ohms)
1
2
3
4
Time (usec)
o: Shot (10/A/17)
x: Shot (11/A/17)

Figure 17

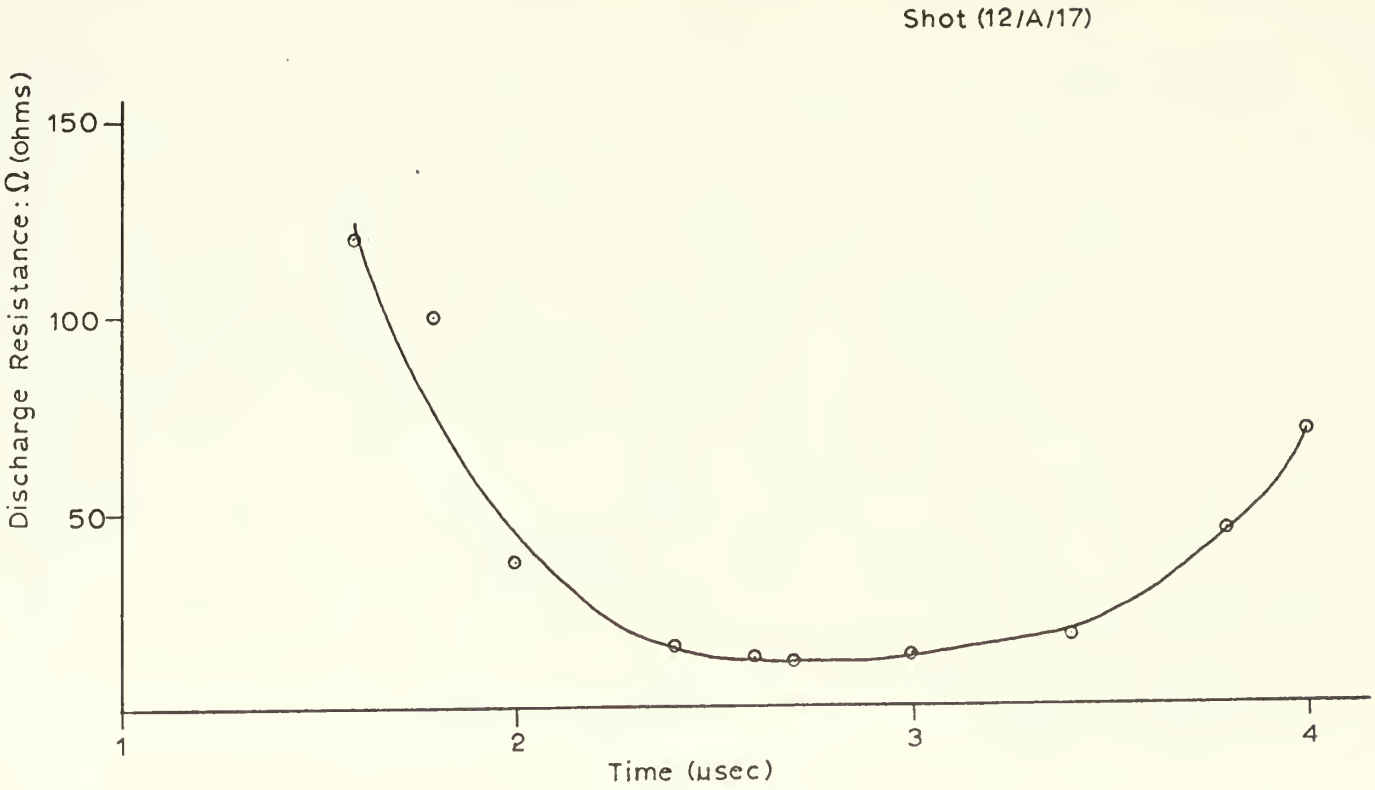
Shot (12/A/17)
Discharge Resistance: Ω (ohms)
150
100
50
1
2
3
4
Time (μsec)

Figure 18

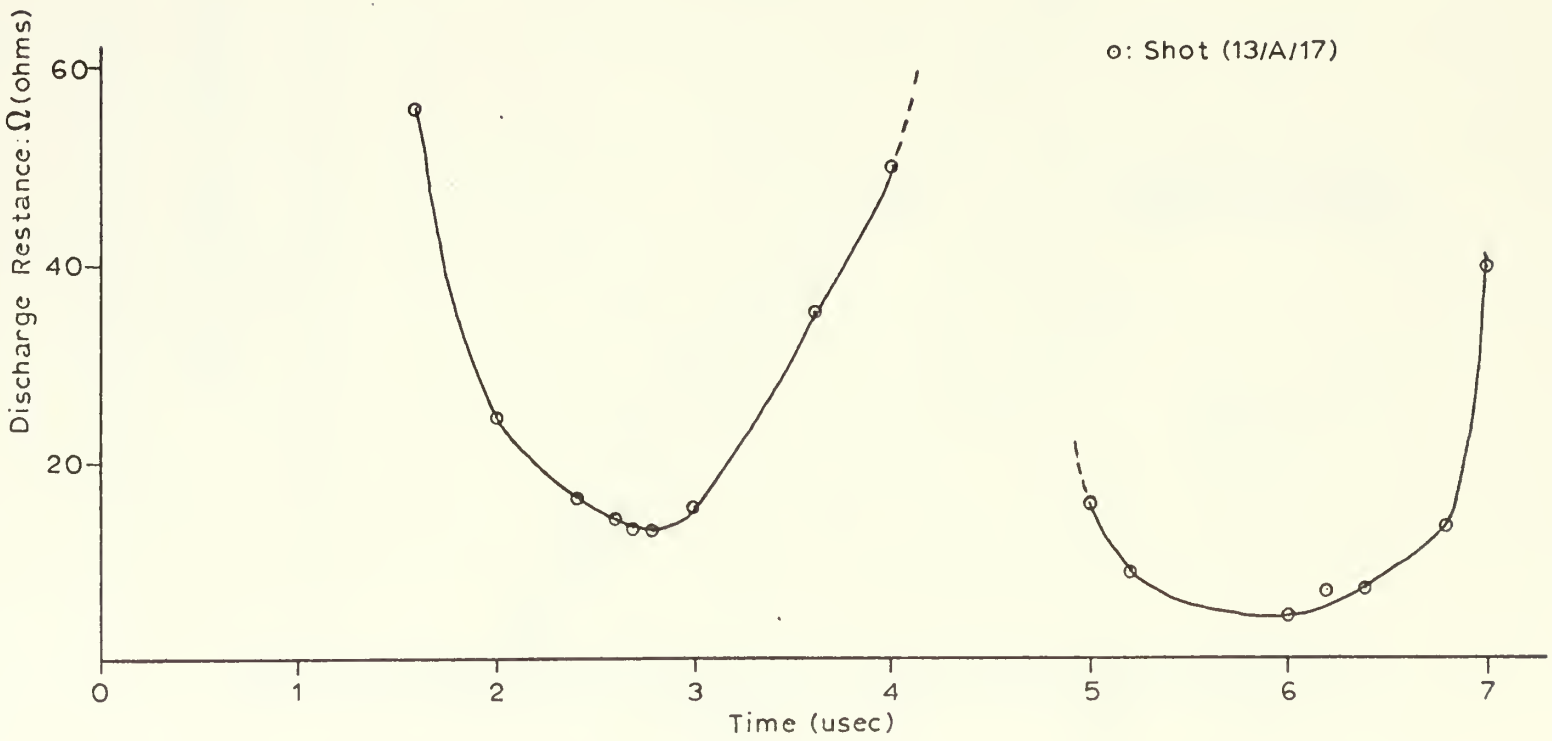
Discharge Restance: Ω (ohms)
60
40
20
0
1
2
3
4
5
6
7
Time (usec)
o: Shot (13/A/17)

Figure 19

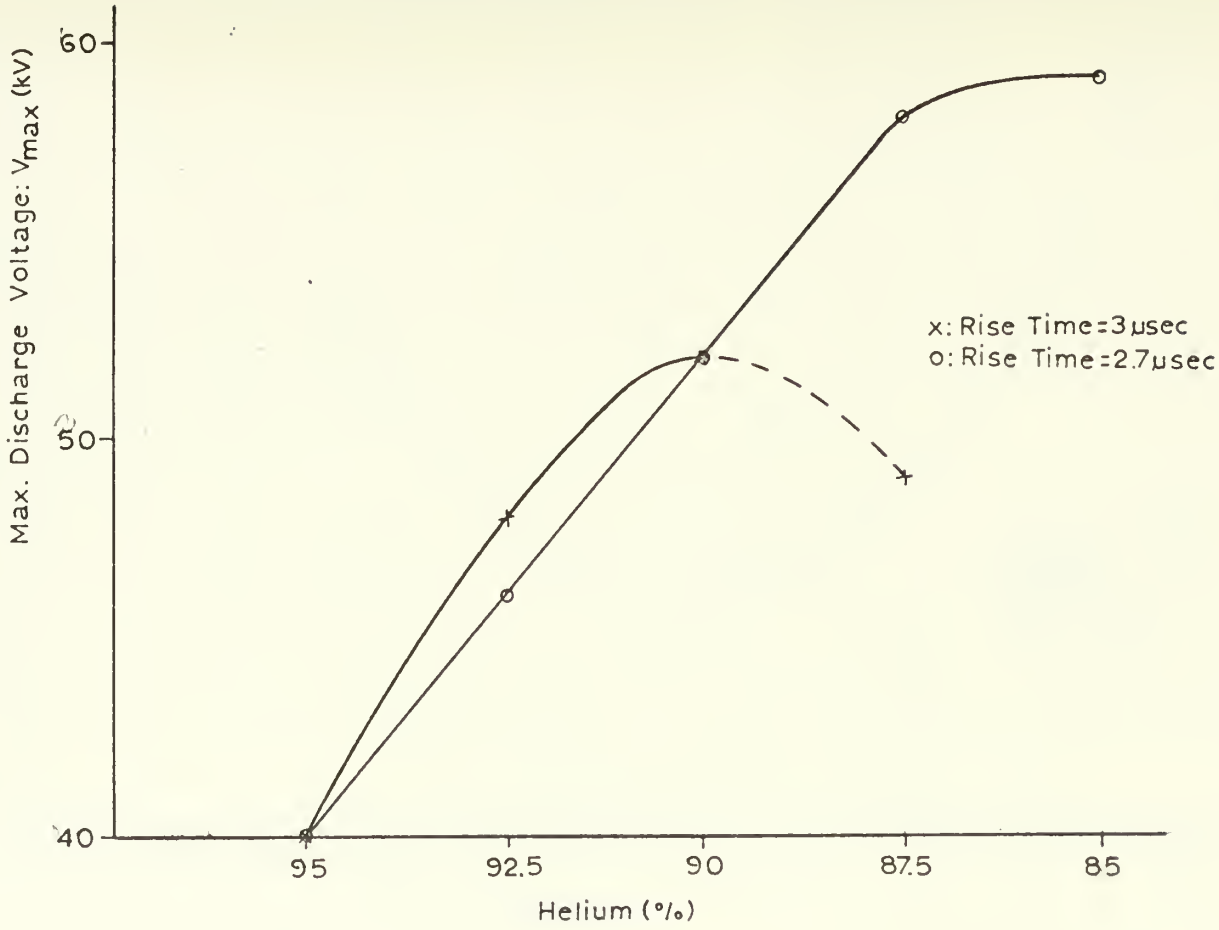
Max. Discharge Voltage: V_{max} (kV)
60
50
40
95
92.5
90
87.5
85
Helium (%)
x: Rise Time=3μsec
o: Rise Time=2.7μsec

Figure 20

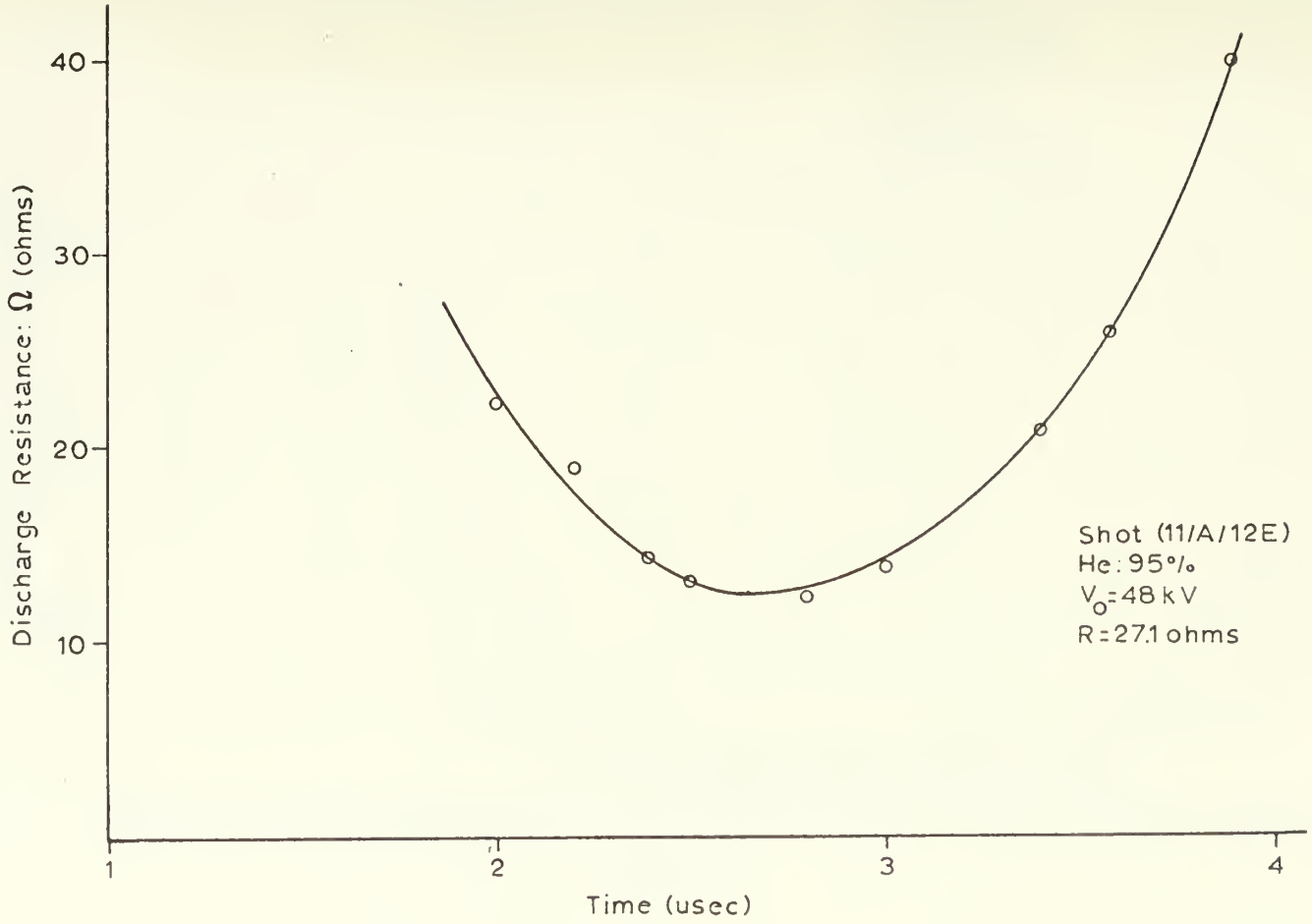
Discharge Resistance: Ω (ohms)
40
30
20
10
1
2
3
4
Time (usec)
Shot (11/A/12E)
He: 95%
V_o=48 kV
R=27.1 ohms

Figure 21

x: Shot (7/A/17)
He = 90%
V_o = 54 kV
R = 25.8 ohms
o: Shot (17/A/17)
He = 85%
V_o = 54 kV
R = 25.5 ohms

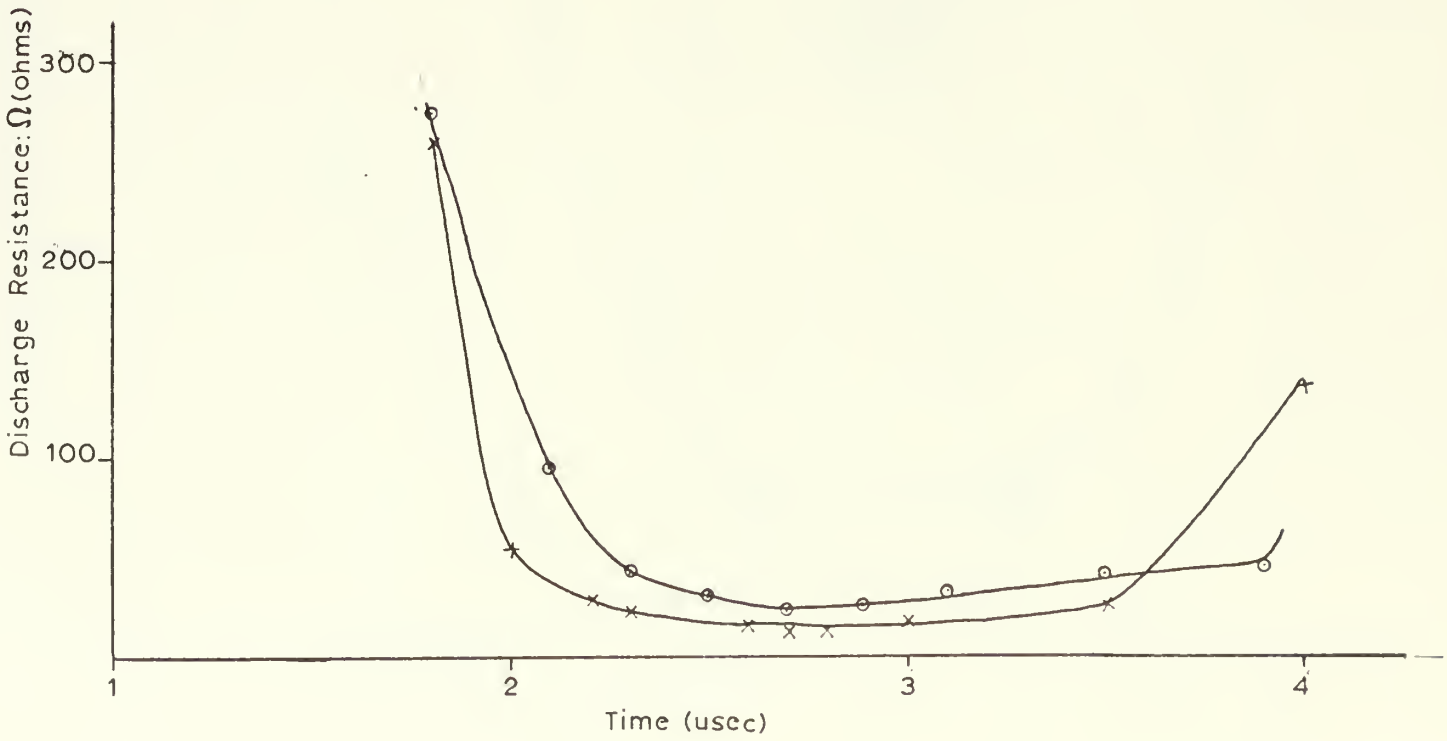

Figure 22

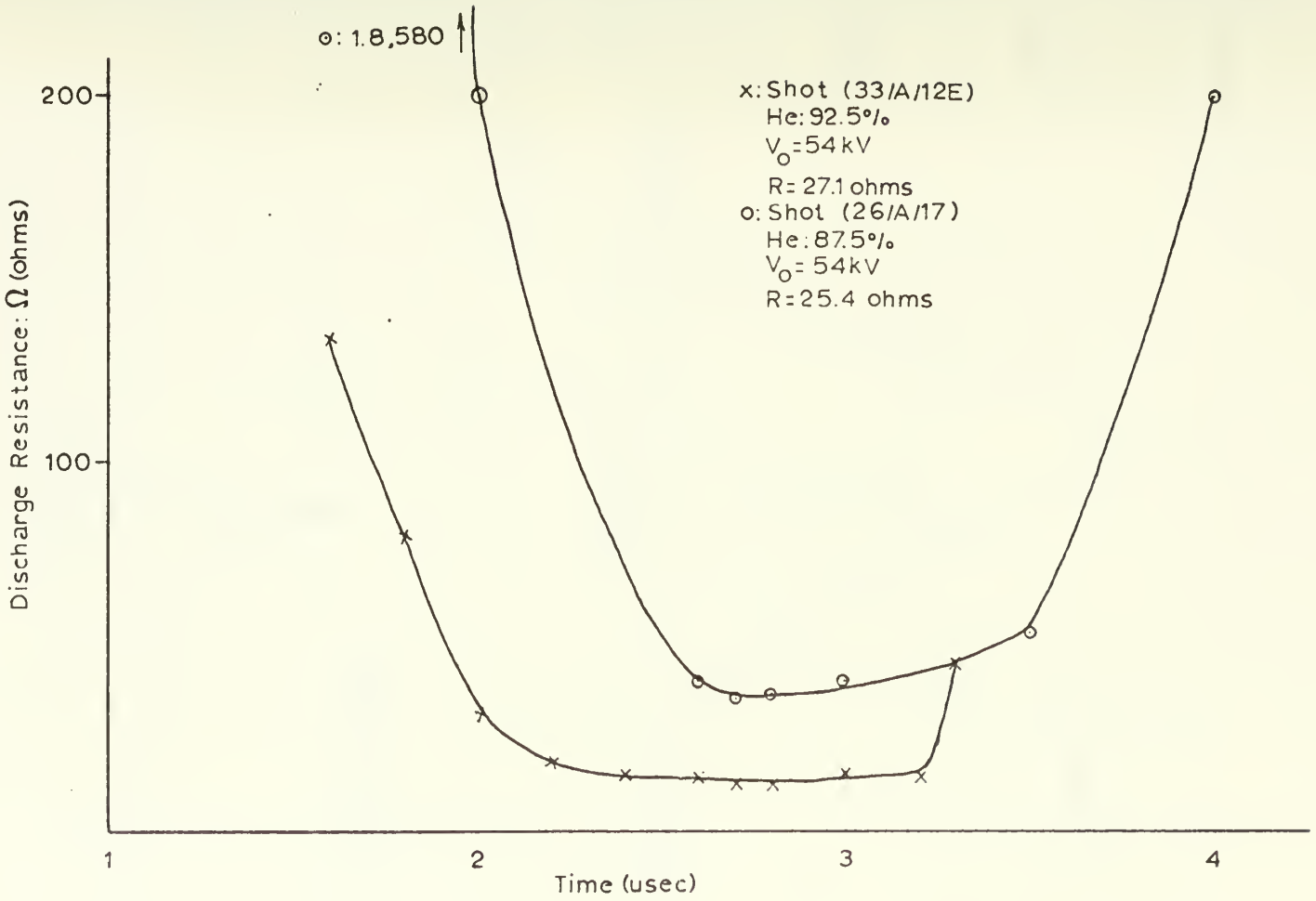
⊙: 1.8,580
x: Shot (33/A/12E)
He: 92.5%
V_o = 54 kV
R = 27.1 ohms
o: Shot (26/A/17)
He: 87.5%
V_o = 54 kV
R = 25.4 ohms
Discharge Resistance: Ω (ohms)
200
100
1
2
3
4
Time (usec)

Figure 23

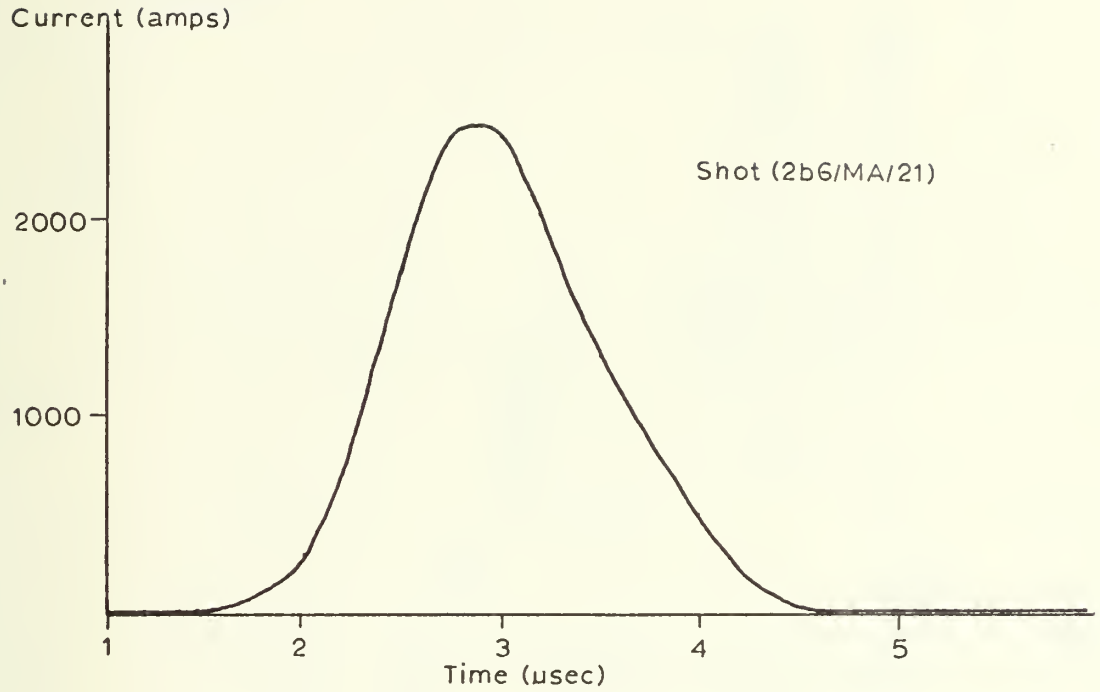
Current (amps)
2000
1000
Shot (2b6/MA/21)
1
2
3
4
5
Time (μsec)

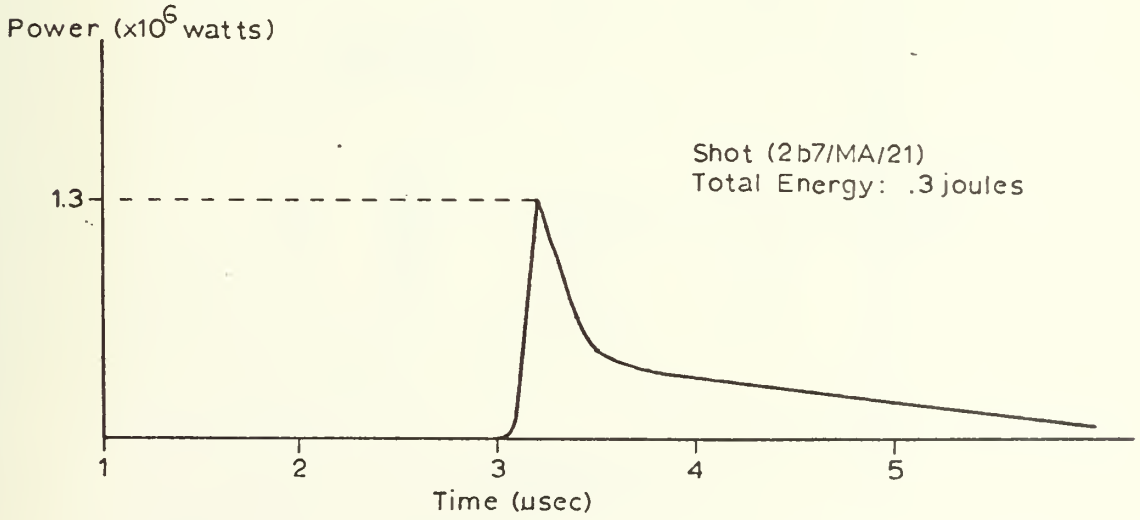
Power (x10^6 watts)
1.3
Shot (2b7/MA/21)
Total Energy: .3 joules
1
2
3
4
5
Time (μsec)

Figure 24

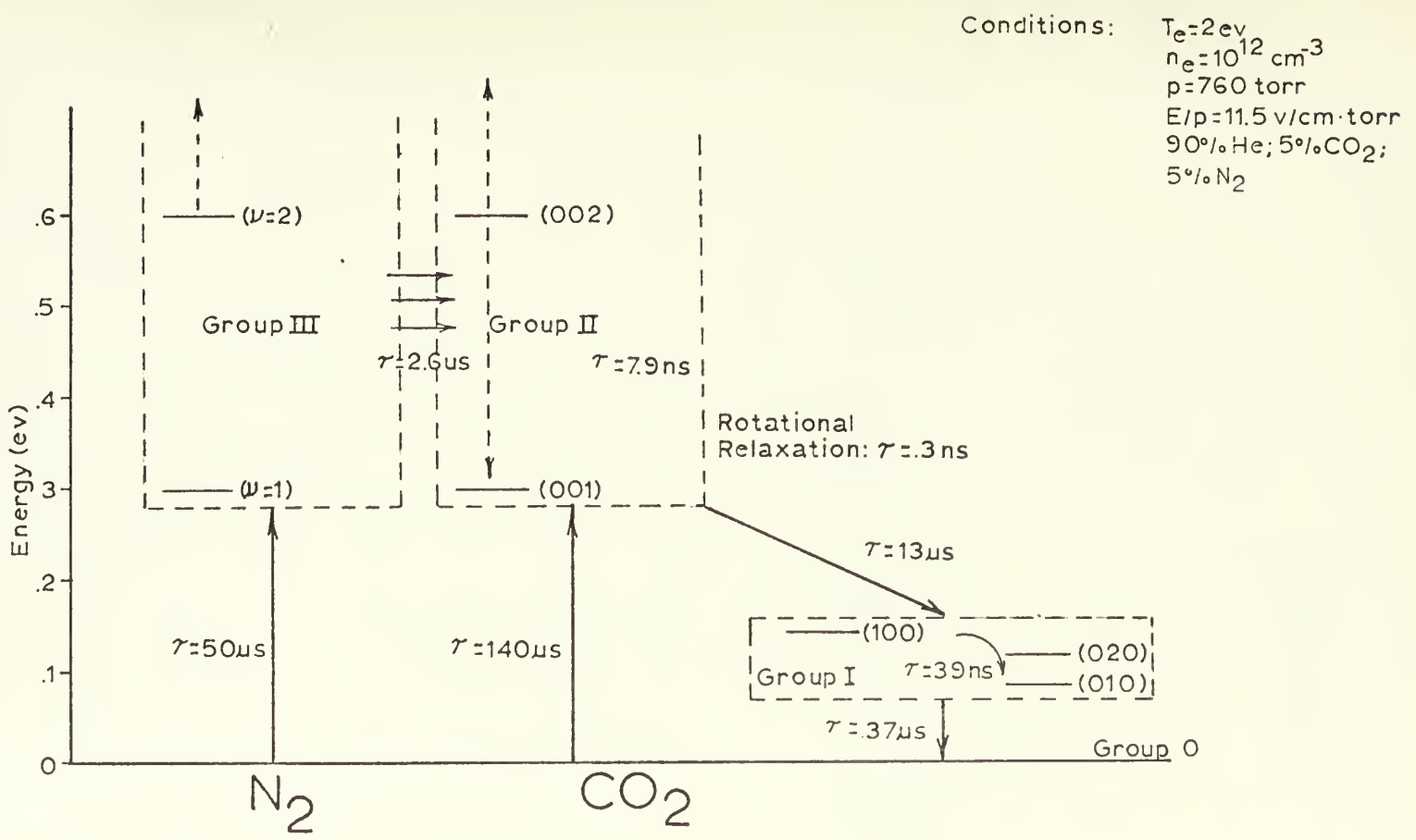
Conditions:
T_e=2ev
n_e=10^{12} cm^{-3}
p=760 torr
E/p=11.5 v/cm·torr
90% He; 5% CO_2;
5% N_2
Energy (ev)
.6
.5
.4
.3
.2
.1
0
(v=2)
(002)
Group III
Group II
τ=2.6μs
τ=7.9ns
Rotational
Relaxation: τ=.3ns
(v=1)
(001)
τ=13μs
τ=50μs
τ=140μs
(100)
(020)
Group I
τ=39ns
(010)
τ=.37μs
Group 0
N_2
CO_2

Figure 25

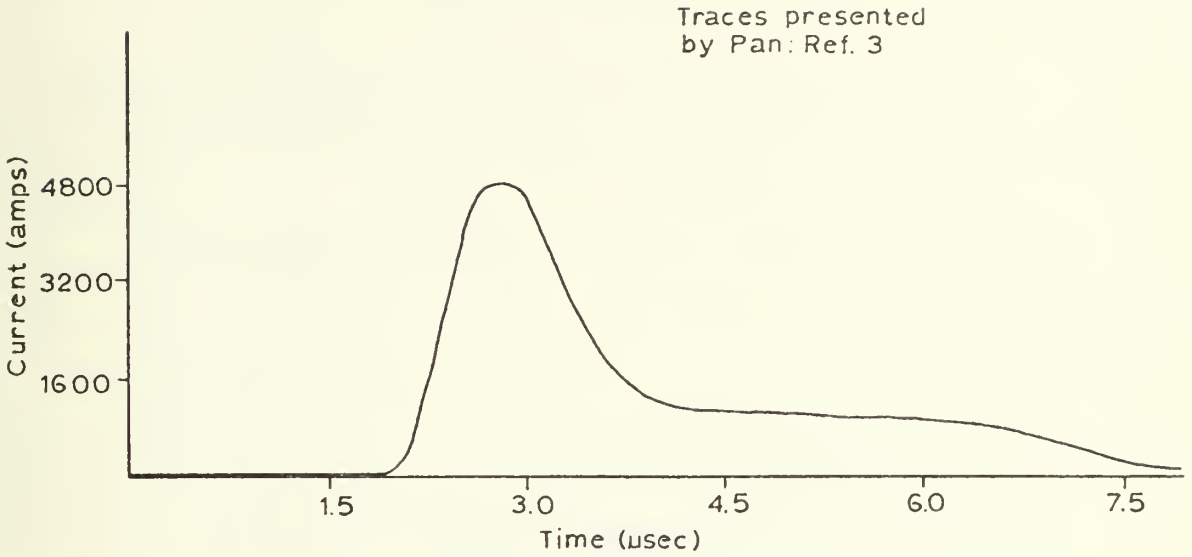
Traces presented
by Pan: Ref. 3
Current (amps)
4800
3200
1600
1.5
3.0
4.5
6.0
7.5
Time (μsec)

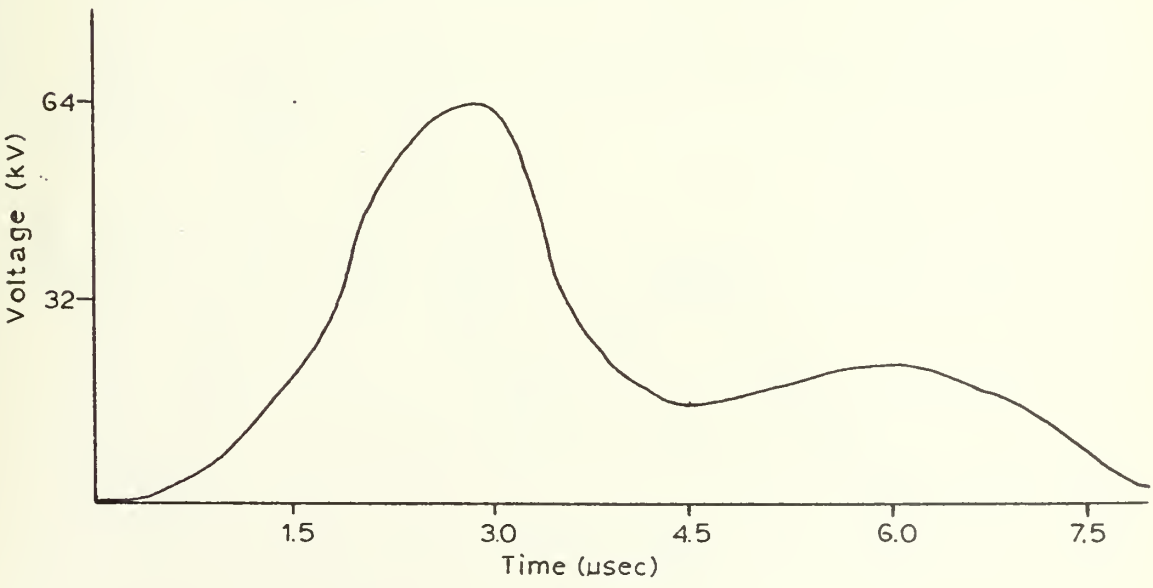
Voltage (kV)
64
32
1.5
3.0
4.5
6.0
7.5
Time (μsec)

Figure 26

Traces obtained for
lasing condition (3/MA/14)

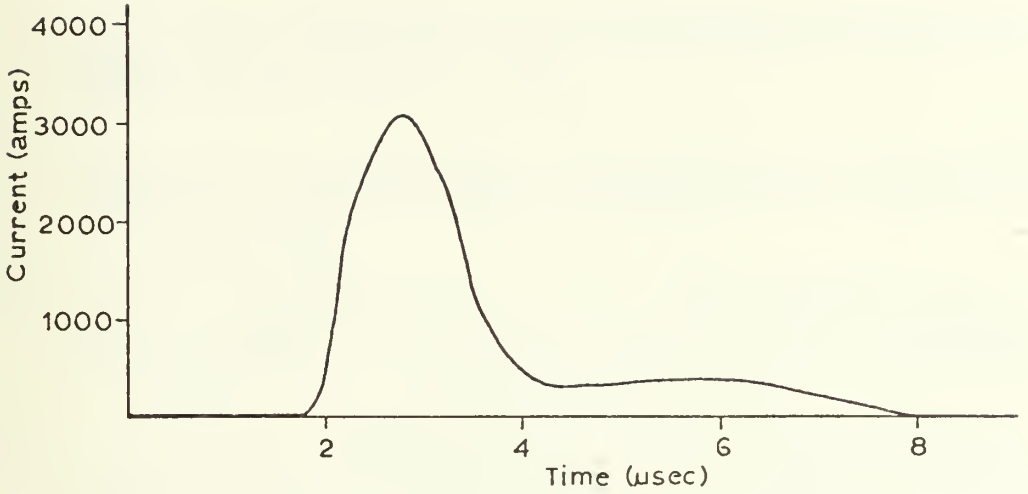

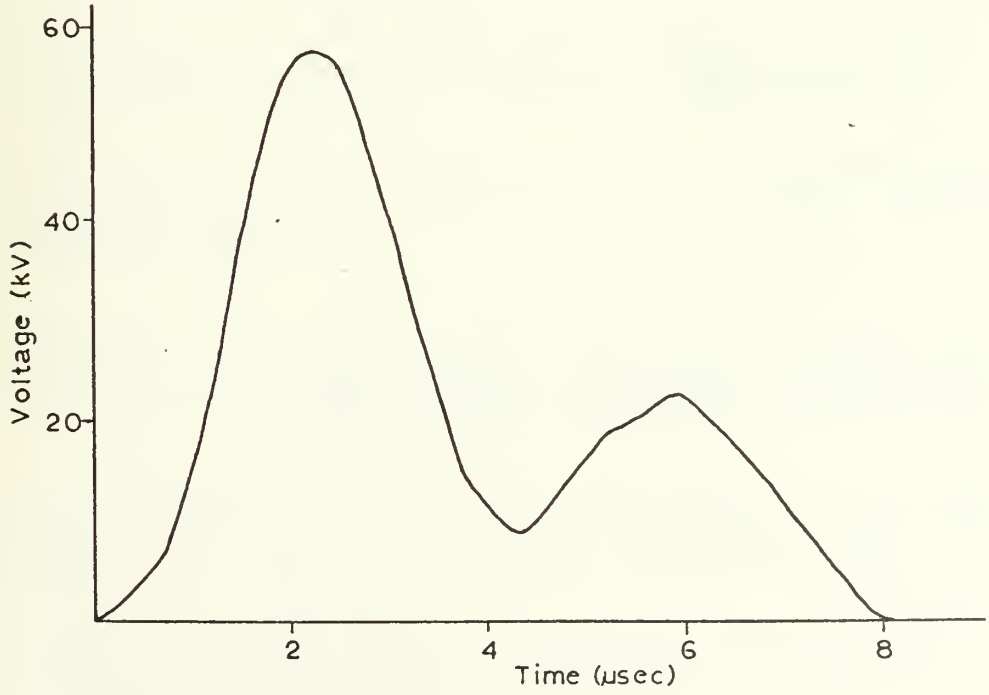

Figure 27

LIST OF REFERENCES

1. Barr, D. H., Construction of a Carbon Dioxide TEA Laser, Master Thesis, Naval Postgraduate School, Monterey, California, 1972.

2. Bishop, R. F., Discharge Characteristics of a Carbon Dioxide TEA Laser, Master Thesis, Naval Postgraduate School, Monterey, California, 1972.

3. Pan, Y. L., Bernhardt, A. F., and Simpson, J. R., "Construction and Operation of a Double-Discharge TEA CO_2 Laser," The Review of Scientific Instruments, v. 43, No. 4, p. 662-666, April 1972.

4. Wolfe, W. L., Handbook of Military Infrared Technology, Office of Naval Research, Department of the Navy. Available from the U. S. Government Printing Office, Washington, D. C., 1965.

5. Oriel Optics Corporation, "Instruments and Components for Optical Research, 1971."

6. Hudson, R. D. Jr., Infrared Systems Engineering, p. 217, Wiley, 1969.

7. Laurie, K. A., and Hale, M. M., "A Pin-Electrode Atmospheric Pressure CO_2 Laser," IEEE Journal of Quantum Electronics, p. 530-531, November 1971.

8. Rampton, D. T., and Gandhi, O. P., "Performance Characteristics of a Helical TEA CO_2 Laser," Applied Physics Letters, v. 21, No. 10, p. 457-460, 15 November 1972.

9. Pearson, P. R., and Lamberton, H. H.,"Atmospheric Pressure CO_2 Lasers Giving High Output Energy Per Unit Volume," IEEE Journal of Quantum Electronics v. QE-8, No. 2, p. 145-149, February 1972.

10. Wynn-Williams, C. E., "An Investigation into the Theory of the Three-Point Gap," Philosophical Magazine, v. 1, No. 2, p. 353-378, February 1926.

11. Meek, J. M. and Loeb, L. B., The Mechanism of the Electric Spark, Stanford University Press, 1941.

12. Dumanchin, R., and others, "Extension of TEA CO_2 Laser Capabilities," IEEE Journal of Quantum Electronics, v. QE-8, No. 2, p. 163-165, February 1972.

13. Deutsch, T. F., "Effect of Hydrogen and CO_2 TEA Lasers," Applied Physics Letters, v. 20, No. 8, p. 315-316, 15 April 1972.

14. Gregoriu, C. and Brinkschulte, H., "A Reliable High Efficiency Atmospheric Pressure CO_2 Laser," Physics Letters, v. 42A, No. 5, p. 347-348, 1 January 1973.

INITIAL DISTRIBUTION LIST

		No. Copies
1.	Defense Documentation Center Cameron Station Alexandria, Virginia 22314	2
2.	Library, Code 0212 Naval Postgraduate School Monterey, California 93940	2
3.	Associate Professor Fred R. Schwirzke Code 61Sw Department of Physics and Chemistry Naval Postgraduate School Monterey, California 93940	2
4.	Assistant Professor Natale M. Ceglio Code 61Cl Department of Physics and Chemistry Naval Postgraduate School Monterey, California 93940	5
5.	Lieutenant William F. Bassett, USN 9281 Hickory Street Norfolk, Virginia 23503	1

Security Classification

DOCUMENT CONTROL DATA - R & D

(Security classification of title, body of abstract and indexing annotation must be entered when the overall report is classified)

ORIGINATING ACTIVITY (Corporate author)

Naval Postgraduate School
Monterey, California

2a. REPORT SECURITY CLASSIFICATION

Unclassified

2b. GROUP

REPORT TITLE

Investigation and Operation of a Carbon Dioxide TEA Laser

DESCRIPTIVE NOTES (Type of report and, inclusive dates)

Master's Thesis; June 1973

AUTHOR(S) (First name, middle initial, last name)

William F. Bassett

REPORT DATE	7a. TOTAL NO. OF PAGES	7b. NO. OF REFS
June 1973	100	14

CONTRACT OR GRANT NO.

PROJECT NO.

9a. ORIGINATOR'S REPORT NUMBER(S)

9b. OTHER REPORT NO(S) (Any other numbers that may be assigned this report)

DISTRIBUTION STATEMENT

Approved for public release; distribution unlimited.

SUPPLEMENTARY NOTES

12. SPONSORING MILITARY ACTIVITY

Naval Postgraduate School
Monterey, California 93940

ABSTRACT

Lasing has been achieved at 10.6 microns using a double discharge CO_2 TEA configuration. The double discharge configuration utilizes three electrodes. The third, "trigger," electrode in this particular device consists of glass encapsulated nichrome wires. The third electrode is responsible for corona formation--the dominant preionization mechanism. A parametric analysis of the discharge was conducted. The discharge was found to be dependent on the gas mixture, the gas flow rate, the voltage rise time and the voltage pulse shape. It was found that satisfactory discharge operation leading to lasing was limited to a very small region of parameter space having a helium percentage of not less than 90% (with 5% CO_2 and 5% N_2), and a rise time on the order of 3 μsec. Lasing action yielded 5 joules/pulse. The energy was limited by the optical components used, and it is felt that the energy can be increased to approximately 18 joules/pulse using different circuit parameters in conjunction with improved optical components.

DD FORM 1 NOV 68 1473 (PAGE 1)

0101-807-6811

Security Classification

A-31408

KEY WORDS	LINK A		LINK B		LINK C	
	ROLE	WT	ROLE	WT	ROLE	WT
TEA Laser						
Carbon Dioxide Laser						
Transverse Excitation						
Pulsed Power						
Infrared Radiation						
Double Discharge Laser